processes

MDPI

Article

Advancing Geothermal Energy Recovery Through Reactive Transport Modelling and Horizontal Well Analysis: A Case Study of Lithuanian Reservoirs

Abdul Rashid Abdul Nabi Memon and Mayur Pal *

Department of Mathematical Modelling, Kaunas University of Technology, 44249 Kaunas, Lithuania; abdmem@ktu.lt

* Correspondence: mayur.pal@ktu.lt; Tel.: +370-612-95-386

Abstract

The study underpins the geothermal energy potential of Cambrian reservoirs in Lithuania, which utilizes the use of reactive transport modelling to examine how different reinjection temperatures and flow rates affect mineral changes. The results are then applied to design field development plans, using petroleum engineering methods such as horizontal wells and induced fracturing. The research study indicates that there are some changes in porosity and permeability over time due to mineral dissolution and precipitation because of injection rates, but no adverse effect of re-injection temperature was observed. Hence, a reinjection temperature of 40 °C is geochemically stable and suitable for long-term operation, with no significant effect on mineral behavior. Moreover, application of horizontal wells proves that there is a significant increase in water production and power (thermal) output due to improved reservoir exposure. Hydraulic fracturing further enhanced the performance and flow rates, concluding that, among all the sites studied, Nausodis demonstrated the highest thermal output, while Genciai showed the lowest potential due to limited reservoir temperature and productivity. Thus, research aims to improve power output by studying how well design, reinjection methods, and chemical reactions affect the reservoir, and it shows that using horizontal wells, fracturing, and proper reinjection temperature can help increase geothermal energy recovery in Lithuania.

Keywords: Cambrian; Devonian; horizontal wells; geothermal; reactive transport modelling; reservoirs

Academic Editor: Wei Liu

Received: 8 December 2025
Revised: 25 December 2025
Accepted: 4 January 2026
Published: 7 January 2026

1. Introduction

It is predicted that Earth's temperature will rise by about 1.5 °C. To fight climate change, the European Union and other countries aim to become climate neutral by 2050. Renewable energy can help reduce emissions, but sources like solar and wind are weather-dependent. Geothermal energy has an advantage because it can provide uninterrupted source of energy to produce electricity and can also be used for district heating purposes, which is useful in cold countries like Lithuania. Lithuania plans for 45% of its electricity from geothermal power [1]. The country has unused geothermal potential, especially in the southwest, where underground temperatures rise faster than normal due to hot granitoid rocks buried under thick sediment layers. Lithuania has three hydrothermal complexes with Cambrian reservoirs, which are currently being used for hydrocarbon production, which is declining fast.

In our previous study [2], we provided a detailed overview of geothermal energy in Lithuania. Another study [1] described the workflow, the geothermal model, and the heat that could be produced using vertical wells from the Cambrian aquifer. Later, we improved energy output by using horizontal wells instead of vertical ones [3]. Furthermore, a recent study [1] focused on using old, depleted oil and gas wells in the Cambrian rock layers for geothermal energy. These wells were originally drilled for oil and gas starting in 1990. We screened the top five promising sites based on water production, focusing on wells that still produce a lot of hot water. Then, we built models to estimate how much heat could be generated, assuming a re-injection temperature of 55 °C. The study found that wells spaced about 1300 m apart could produce 38 to 187 GWh of heat per year. The Nausodis site had the highest potential (187 GWh) because it has thick rock layers and a high Net-to-Gross ratio. Diegliai, Vilkyčiai, and Siupariai also showed good potential. The Genciai site had lower potential (38,400 MWh) due to cooler rocks and lower water production rates [1,4]. This article revisits these sites to maximize heat production using re-injection water temperature.

The consideration of re-injection water temperature was necessary because the energy production is a function of change in temperature between produced and injected water [5–8]. In this study, we have looked at the effects of re-injection temperature. First, we have analyzed the effect of re-injection of high saline on mineral precipitation and dissolution using reactive transport modelling, and then we revisited the plan using horizontal wells to maximize the power production.

In our previous studies [1–4], we demonstrated that the Cambrian reservoir's relatively low porosity and permeability significantly limit the water production capacity of existing vertical wells. Consequently, this work extends the analysis to evaluate the use of horizontal wells as a means of enhancing water production and improving the overall performance of the geothermal system.

Thus, the paper is organized as follows: First, we introduce the geological site and present the characterization of the Cambrian reservoirs and their properties. Research data gaps are highlighted in the next section. Next, we introduce the reactive transport modelling approach, which is used to test the impact of geothermal fluid on the reservoir properties. Subsequently, we proposed the field development plan of the screened sites using horizontal wells. The outcome of the modelling approach used in reference [1] is applied along with the hydrocarbon practice for evaluating high, mid, and low cases for predicting average water production rates. Finally, we estimated the theoretical power that can be obtained by the applying changes of the reactive transport modelling and field development plan for all selected sites. The main conclusions are then summarized.

2. Geology of Cambrian Reservoirs

The Cambrian formation is one of the largest geological layers in the Baltic region, covering Lithuania, Latvia, Estonia, Belarus, the Kaliningrad region, Poland, and the Baltic Sea. It is an important zone for hydrocarbon exploration because it has good reservoir properties (see Figure 1). The rocks were formed in shallow seas and included sandstones, siltstones, and argillites. In Lithuania, the depth ranges from 300–500 m in the east to 2200–2300 m in the west, and the thickness increases from 90–100 m to 170–250 m offshore. Moreover, the Deimena Group sandstone is the most important reservoir unit in the Cambrian system. Quartz is the main mineral, but the rock also contains feldspar, clay, carbonates, pyrite, apatite, and other minerals. Many minerals formed later and act as cement. The sandstone's quality depends on how quartz cement is distributed. Poor grain sorting and clay reduce permeability. Apatite coatings can block quartz growth.

Kaolinite and iron-rich dolomite also appear. Porosity and permeability vary widely across the formation.

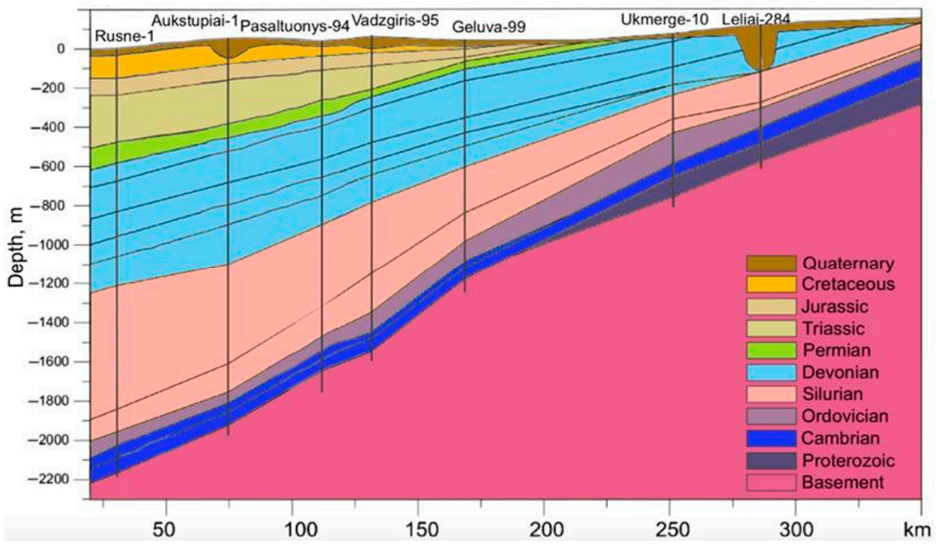

Figure 1. Generalized geological cross-section throughout Lithuanian territory [1].

The Cambrian layer forms the base of the Baltic Basin's sedimentary rocks and rests on the older Precambrian basement. These sands, silts, and clays were deposited in shallow seas. Cambrian rocks appear at the basin's edges, while thickness increases toward Southwest Poland, reaching about 5 km. This formation is important for hydrocarbons and understanding regional geology. More information about the geology and mineral specification can be found in reference [1,4].

Drilling and completing wells are very expensive in geothermal projects, often costing 30–40% of the total budget. A good solution is to reuse abandoned oil and gas wells, since they already provide subsurface data. In West Lithuania, Cambrian sandstone oil fields have detailed studies and depleted wells, making them good candidates for geothermal use. Up to 19 reservoirs were included in the initial screening (see Table 1). First, we identified sites with the highest amount of water extracted since the start of production [1]. Water production data were collected from reports held by the Lithuanian Geological Survey and from Lithuanian companies upon request (e.g., Klaipeda Energy and Minijos Nafta). The presence of water production infrastructure was an important selection factor. A higher number of wells increases the chance of extracting more water. The screening process resulted in a list of the five most promising geothermal sites (see Table 2). Subsequently, the petrophysical properties of each site were characterized, including porosity, permeability, depth, average subsurface temperature, water salinity, injection water temperature, reservoir pressure, expected flow rates, reservoir thickness, and net-to-gross ratio (NTG). The property ranges were derived from oil exploration reports submitted by operating companies to the Lithuanian Geological Survey [1]. These sites were then used for a detailed analysis, which included uncertainty modeling of both dynamic and static parameters. A probabilistic forecasting approach was applied to estimate the geothermal energy production potential of the selected sites. This study aims to be a benchmark for evaluating geothermal potential in similar reservoirs in Lithuania, Latvia, Kaliningrad, and Poland. More details about the screening and methodology are provided in reference [1].

Table 1. Water production history from all oil reservoirs [1].

Oil Reservoir	Water Extracted from the Field Since the Start of Production, m^3	Water Produced in 2022, m^3/y	No. of Wells	Temperature at the Top of Cambrian, °C
Genciai	5,651,869.915	86,236.001	10	74
Vilkyciai	4,129,050.971	64,714.905	15	85.5
South Siupariai	2,955,872.771	0	10	83
Nausodis	2,107,141.674	42,946.523	14	75
Diegliai	1,623,752.633	0	6	82.9
Kretinga	1,319,346.659	8488.2	9	70.2
Siupariai	872,572.994	372.661	6	76.3
Pociai	559,226.701	8377.844	5	84.3
Vezaiciai	543,463.32	10,453.455	12	76
Girkaliai	370,381.596	8571.187	6	71.7
Liziai	365,821.766	3949.233	4	
Sakuciai	152,549.824	3843.274	4	84
Ablinga	61,134.015	0	3	80.8
Agluonenai	45,666.05	419.345	2	
Uoksai	10,358.773	0	1	84.3
Silale	3246.94	0	2	82.4
Auksoras	2522.611	0	1	
Zadeikiai	1794.846	0	1	
North Vezaiciai	1221.246	141.685	1	76

Table 2. Petrophysical parameters of the five screened sites [1].

Reservoir Parameters	Genciai	Vilkyciai	South Siupariai	Nausodis	Diegliai
Effective porosity, %	6–8–10	4.6–6.5–9.7	5.4–6.2–7.7	0.3–8–15	6–8.5–11.3
Permeability, mD	0.1–12–219	0.1–10.4–41.4	0.01–16.7–45.14	0.01–9.4–895.6	0.1–10.8–47
Depth, m	1800–1826.4	1975–1992.5	1958–1988	1765–1860.6	1940–1990
Average temperature, °C	73.64	88	83	75	85
Water salinity, mg/L	146,217.33	229,000	-	138,241.18	200,000
Injection water temperature, °C	55	55	55	55	55
Reservoir Pressure, bars	191.66	222	216	190.491	213
Reservoir thickness, m	26.4; 16.19	68; 17.5	30; 16	95.6; 82.28	61; 25
NTG (Net-to-Gross), units	0.61	0.26	0.53	0.86	0.41

3. Identification of Data Gaps

Out of the 19 identified reservoirs, five were selected for detailed geothermal potential analysis. These sites were chosen based on indications of high-water production and elevated reservoir temperatures, which are favorable for geothermal applications. However, several data gaps exist for these reservoirs, limiting a comprehensive assessment of their geothermal potential. These limitations are discussed in detail in the following sections. Despite these challenges, the available data are sufficient to proceed with the analysis and allow meaningful insights to be extracted from the existing information.

Seismic surveys are widely used to investigate geothermal, oil, and mineral resources, as they provide essential information on reservoir depth, geometry, fault structures, and support optimal well placement. Since geothermal energy exploitation relies on subsurface heat, knowledge of rock thermal conductivity is critical. Thermal conductivity varies with mineral composition, porosity, fluid saturation, and grain structure, and these properties govern heat transfer through different geological layers [9].

In addition, well logging during drilling records temperature, pressure, and rock properties at various depths. However, these measurements may be affected by drilling fluids and tool response times, requiring corrections to obtain reliable geothermal and pressure gradients. Well logs and core samples further supply information on porosity, permeability, and grain characteristics, which are essential for understanding reservoir formation and quality. Despite this, such detailed information is not fully available in the present study.

Furthermore, dynamic data—such as fluid production history, temperature, and pressure variations during reservoir operation—are lacking. In particular, bottom-hole pressure data, which are crucial for evaluating remaining reservoir pressure and well performance, are unavailable [10–21]. In geothermal systems, the reinjection of cooler fluids can also trigger geochemical reactions with reservoir rocks. Accurate prediction of these processes requires detailed fluid and rock property data. Reactive transport and coupled thermo-hydro-mechanical-chemical (THMC) modeling are, therefore, essential tools for understanding heat transport, fluid flow, geochemical interactions, and long-term rock behavior.

Economic analysis is important in geothermal projects because they require high upfront costs and risks. Profitability depends on low operating costs, good ROI and NPV, and a business plan that considers reinjection and long-term closure costs. Together, collecting and correcting all these data types is key to accurately evaluating geothermal resources and designing efficient, safe, and sustainable energy systems. Therefore, Table 3 summarizes the research gaps that are present in our study.

Table 3. Research gaps in the study.

Sr. No	Research Items	Description
1	Seismic (4D)	Nature of reservoir, Temperature front monitoring, Depth & Thickness maps.
2	Thermal conductivity	Heat calculations, Heat Flow.
3	Well logs	Reservoir description, Temperature corrections, Geothermal temperature, and pressure gradient analysis.
4	Core samples	Reservoir Description, Laboratory analysis.
5	Dynamic field data	Production, Temperature, and Bottom hole pressure history for history matching and predictions.
6	Reactive Transport Modelling (RTM)	Mineral changes, study dissolution and precipitation of minerals
7	Thermal-Hydraulic-Mechanical-Chemical (THMC) Modelling	Study mechanical behavior of rocks during production and injection of fluids.
8	Economic Modelling	To develop business case model.

4. Reactive Transport Modelling (RTM) for Cambrian Reservoir

To understand deep subsurface, geology is essential for successful energy projects. Thus, a multi-disciplinary approach is needed, combining geology, geochemistry, and geothermal science. RTM helps simulate fluid flow, minerals, and temperature interaction change, along with fluid composition changes over time. In Cambrian sandstone aquifers, RTM helps explain quartz growth, clay changes, and cementation that affect reservoir

quality. It also predicts long-term mineral and fluid changes during heat extraction and reinjection, helping understand geothermal reservoir behavior and stability.

Thus, reactive transport modelling not only enhances the predictive capability of subsurface models but also supports the development of more sustainable and scientifically informed strategies for resource extraction and subsurface management. In our study, we utilized this RTM technique to study the effect of produced water re-injection temperature. This analysis was carried out on a large scale using TOUGHREACT_rel_V413_exe_011122 simulations [22] through the development of a two-dimensional (2D) model designed to predict how a reservoir evolves over time when saline, different low-temperature water is re-injected. For the same, we defined two scenarios as Model 1 and Model 2, and to study the effect of the injection parameters, we created a 2D radial model with six uniform layers, each 2.4 m thick, extending 1000 m from the injection well, as shown in Figure 2. Initial reservoir properties used in TOUGHREACT simulation for the axis–symmetric model, e.g., porosity and permeability, are shown in Figure 3. The heat transfer between the reservoir and the permeable rocks above and below it is an important process. These confining layers are modelled as endless half-spaces, and the heat exchange is calculated using a semi-analytical method [22]. The model setup can be found in detail in reference [23].

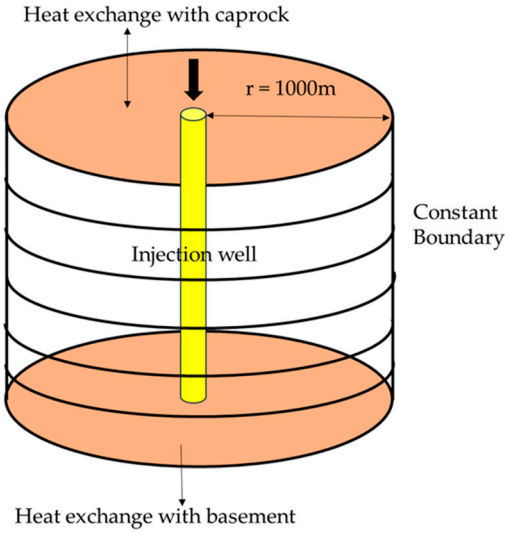

Figure 2. Conceptual representation of the injection well in the Cambrian complex used for TOUGHREACT simulations.

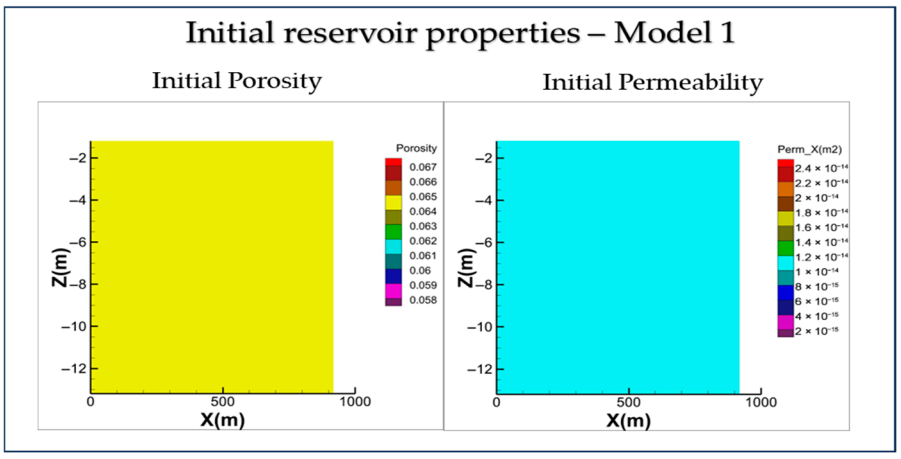

Figure 3. Plots of initial reservoir properties used in TOUGHREACT simulation for the axis–symmetric model 1, porosity, and permeability plots.

The reservoir produced water composition is elaborated in Table 4, and mineral composition, along with reaction parameters, is described in Table 5. While the reservoir properties of Model 1 and Model 2 are described in Table 6. The only difference in both models is the different injection rates because we consider a hypothetical case with a high injection rate to see the effect of injection rate and varying temperatures. The low case injection rate is defined as per the desired rate from the reservoir field development plan (Base case production rate).

Table 4. Primary aqueous composition of Cambrian aquifer.

Component	Ionic Composition (mol/kg of Water)
Ca^{+2}	1.03×10^{-3}
Mg^{+2}	1.66×10^{-6}
Na^{+}	1.27×10^{-1}
Cl^{-}	1.42×10^{-1}
$SiO_2(aq)$	1.22×10^{-2}
HCO^{3-}	1.04×10^{-3}
$So_4{}^{2-}$	2.63×10^{-4}
K^{+}	1.59×10^{-2}
AlO^{2-}	1.08×10^{-5}
Ba^{2+}	1.50×10^{-5}
Sr^{2+}	1.09×10^{-4}
Fe^{2+}	1.02×10^{-2}
NH^{4+}	8.10×10^{-3}
I^{-}	2.83×10^{-3}
Br^{-}	8.26×10^{-1}
$B(OH)_3$	2.00×10^{-2}
$HFeO_2$	2.63×10^{-4}

Table 5. Mineral and reaction parameters for reactive transport modelling.

Minerals	Minerals	Mineral Initial Volume	Rate Constant	Activation Energy
Primary	**Precipitation/Dissolution**	**Fraction**	**(mol/m^2·s)**	**(kJ/mol)**
Anhydrite	Equilibrium	0.000		
Gypsum	Equilibrium	0.000		
Anorthite	Equilibrium	0.131		
Calcite	Kinetic	0.004	1.60×10^{-9}	41.87
Illite	Kinetic	0.054	3.16×10^{-13}	58.6
Quartz	Kinetic	0.654	1.04×10^{-14}	87.7
Kaolinite	Kinetic	0.051	1.78×10^{-13}	58.6
Muscovite	Kinetic	0.000	3.16×10^{-13}	58.6
Dolomite-2	Kinetic	0.020	2.95×10^{-8}	52.2
Celestite	Kinetic	0.000	0.00×10^{0}	0
Barite	Kinetic	0.000	1.26×10^{-8}	30.8
K-feldspar	Kinetic	0.056	3.89×10^{-13}	38
Hematite	Kinetic	0.011	2.51×10^{-15}	66.2

The reactive transport modelling using TOUGHREACT [22] predicts changes in the reservoir's properties—especially porosity and permeability—by comparing the final values to the starting values. This is done using the color scale shown on the right side of each simulation image, which shows how concentrations have changed. In addition, the mineral legend helps explain where minerals have dissolved (shown as negative values) or formed (shown as positive values) during the simulation period. The impact of operating conditions on the reservoir properties is described below.

Table 6. Model properties used for reactive transport modelling.

	Low Case	Hypothetical High Case
Parameters	**Model 1**	**Model 2**
	Reservoir Parameters	
Porosity (%)	6.5	6.5
Permeability (mD)	11	11
Specific heat of rock (J/Kg·°C)	2.4	2.4
Layers	6	6
Thickness of layer (m)	2.4	2.4
Density of water (Kg/m^3)	1129	1129
	Boundary Conditions	
Reservoir Temperature (Produced water temperature) (°C)	88	88
Re-injection water temperature (°C)	55/40/30/20/10	55/40/30/20/10
Water re-injection rate (sm^3/day)	349	5800
	Time Steps	
Simulation Time period (years)	50/40/30/20/10	50/40/30/20/10

4.1. Effect of Time and Re-Injection Temperature on Reservoir Properties of Model 1

In Model 1, the injection rate considered is the base case water production rate of Vilkyčiai field. The results obtained from the RTM are elaborated in Figures 4 and 5. Figures 4 and 5 show that both porosity and permeability change over time, as the amount of mineral dissolution and precipitation in the reservoir also increases from year 0 to year 50. The porosity near the well increases by 6%, and away from the well, (20 m) it decreases by 10%. While permeability near the well increases by 53%, away from the well (20 m), it decreases by 83%. In addition to that, there is no effect of re-injection temperature on porosity and permeability.

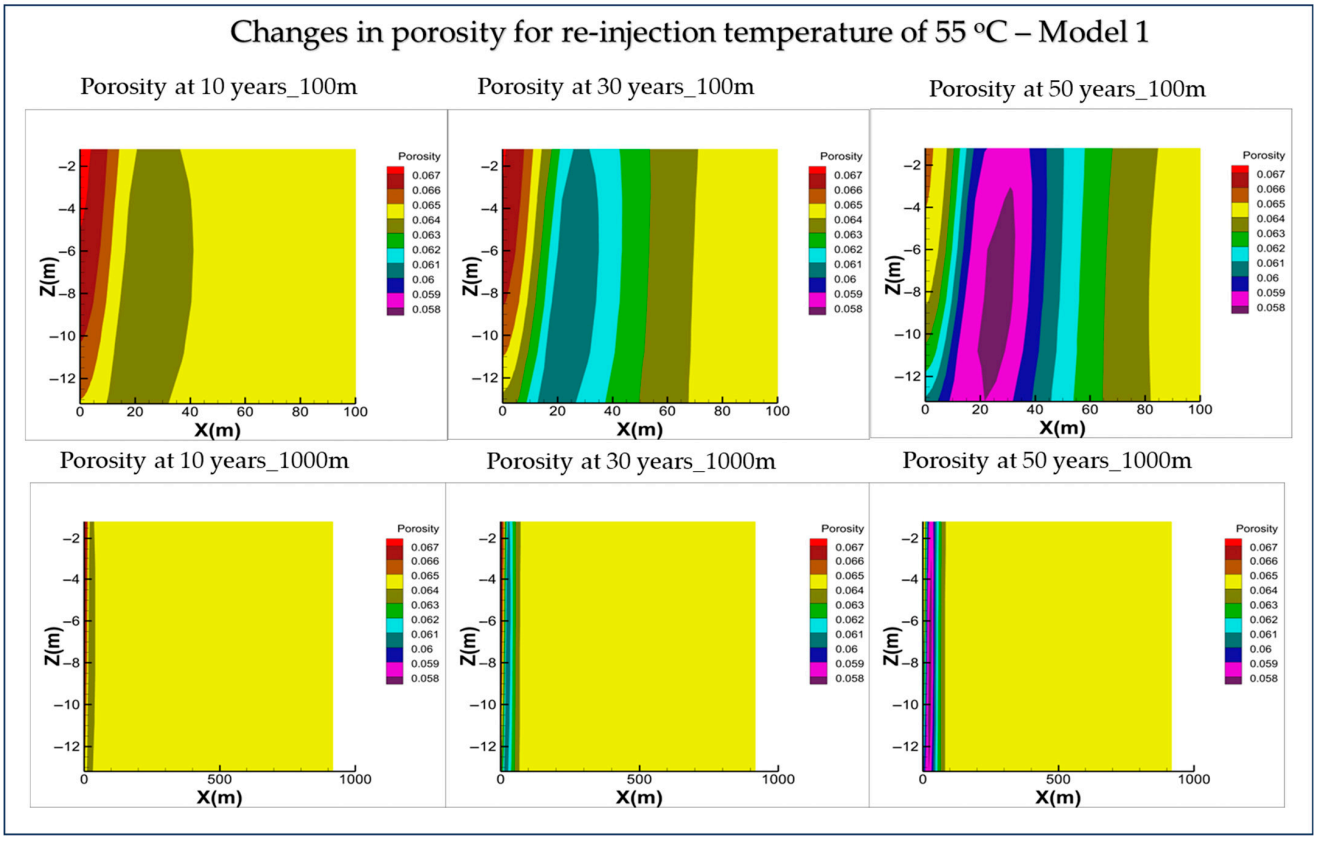

Figure 4. *Cont.*

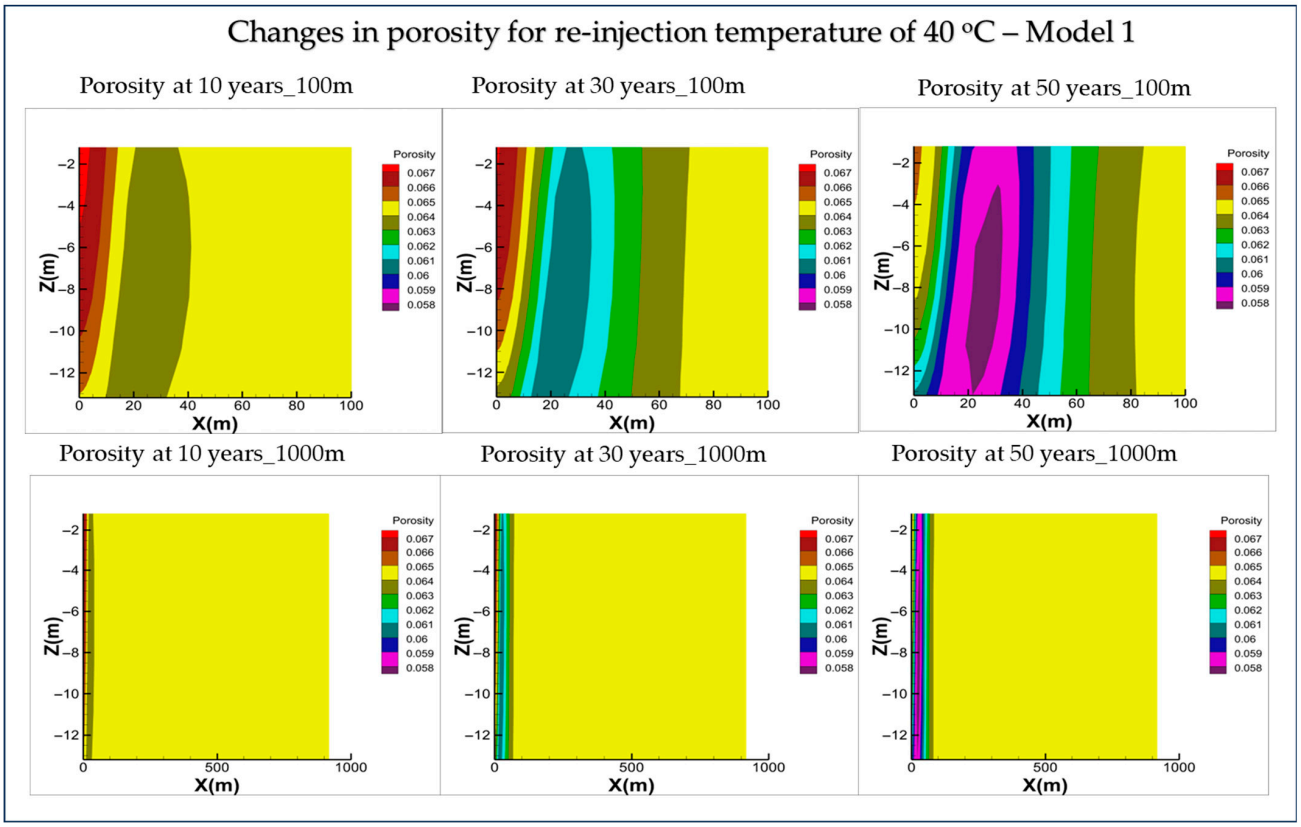

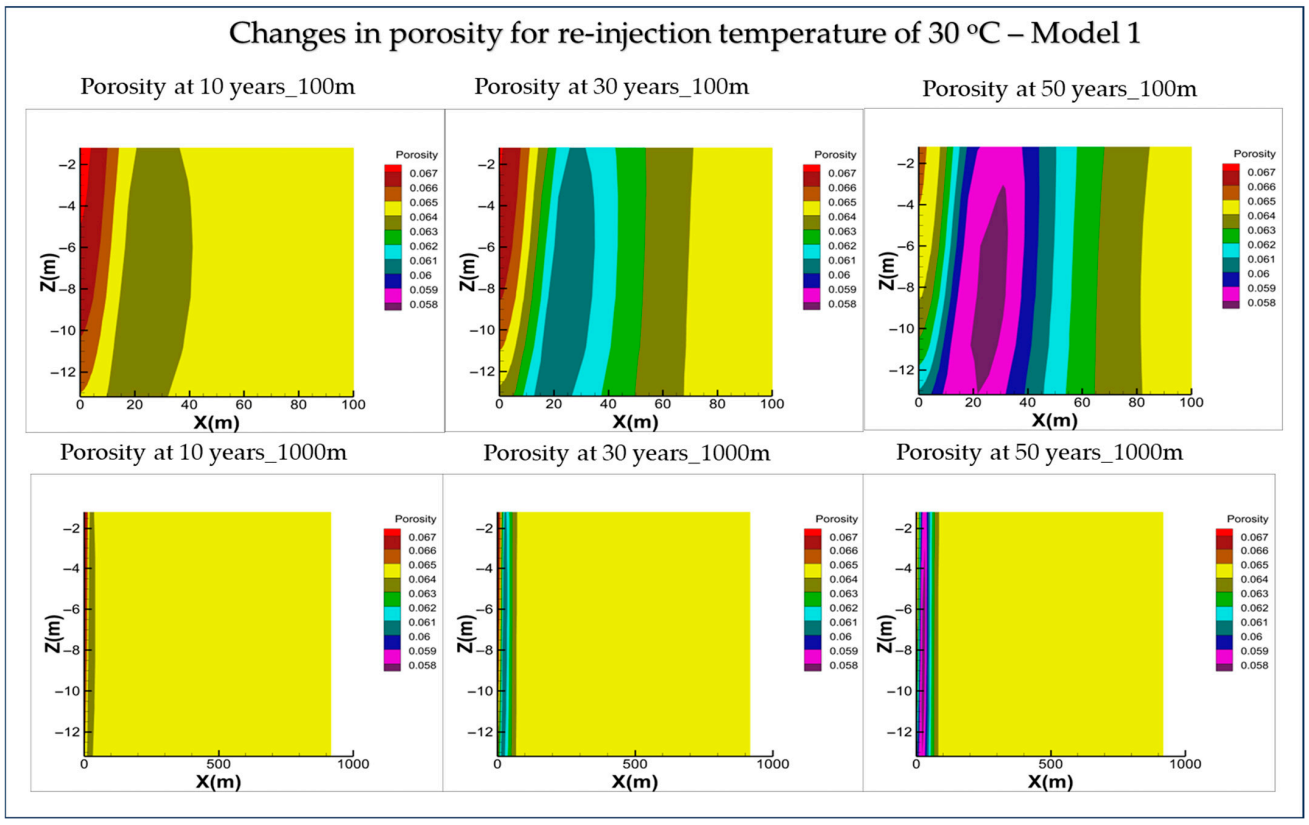

Figure 4. *Cont.*

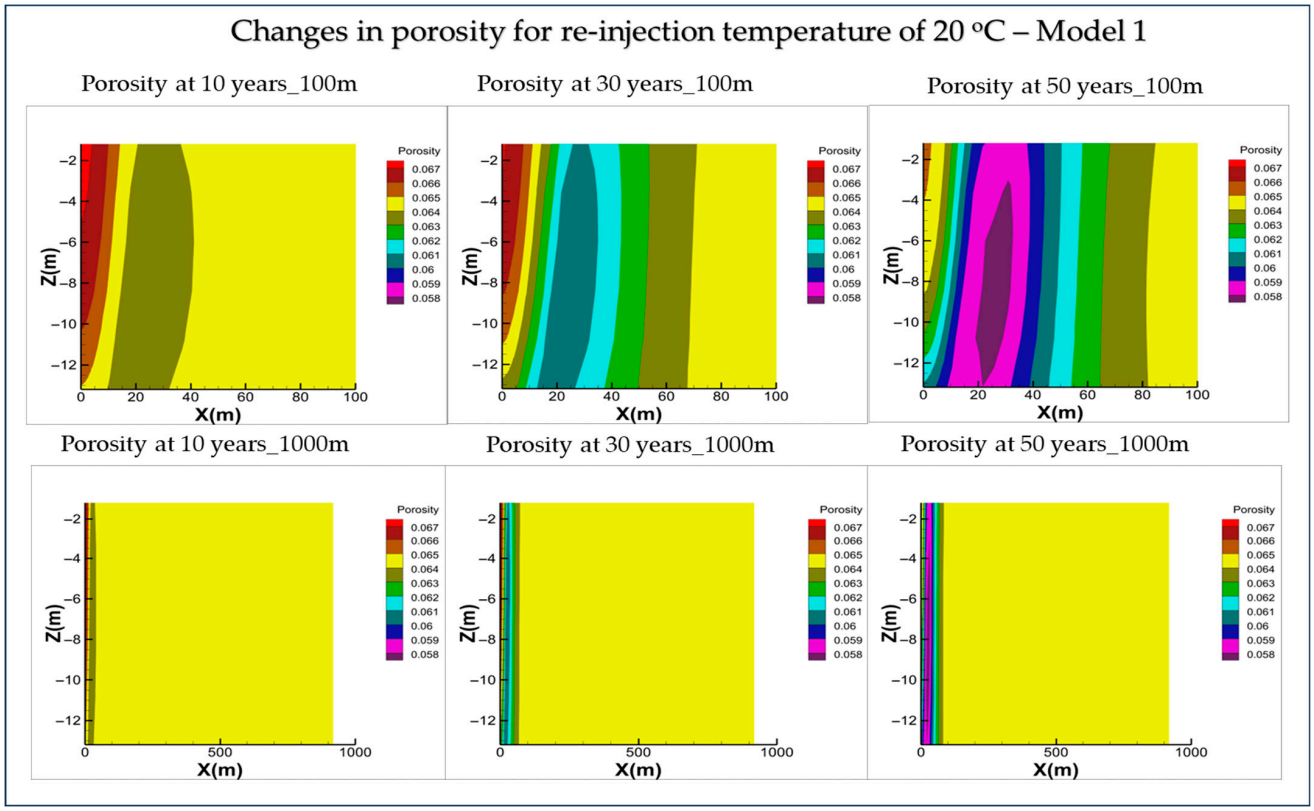

Figure 4. Effect of operation time and injection temperature on reservoir property–porosity of Model 1, changes shown for reservoir porosity at 100 and 1000 m from injection well. Results are shown for 10, 30, and 50 years.

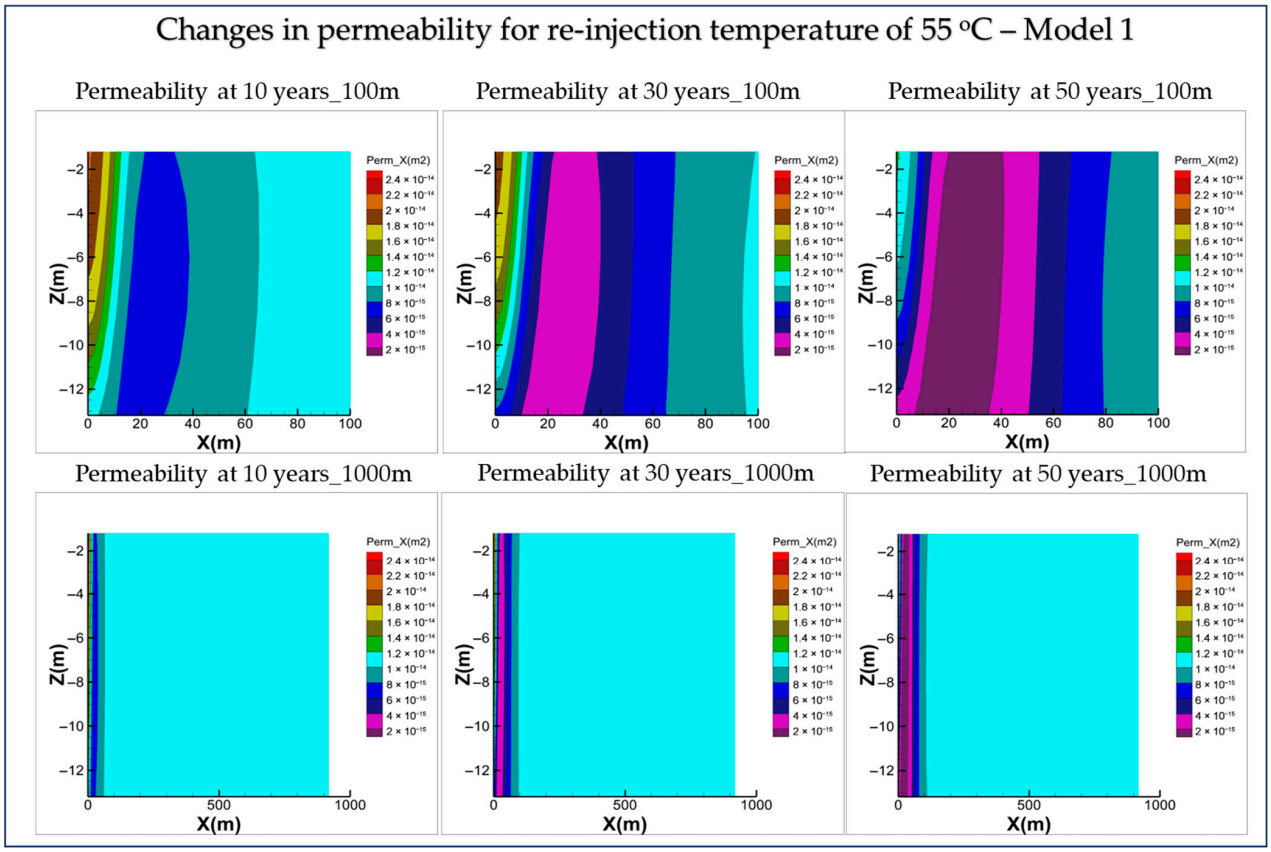

Figure 5. *Cont.*

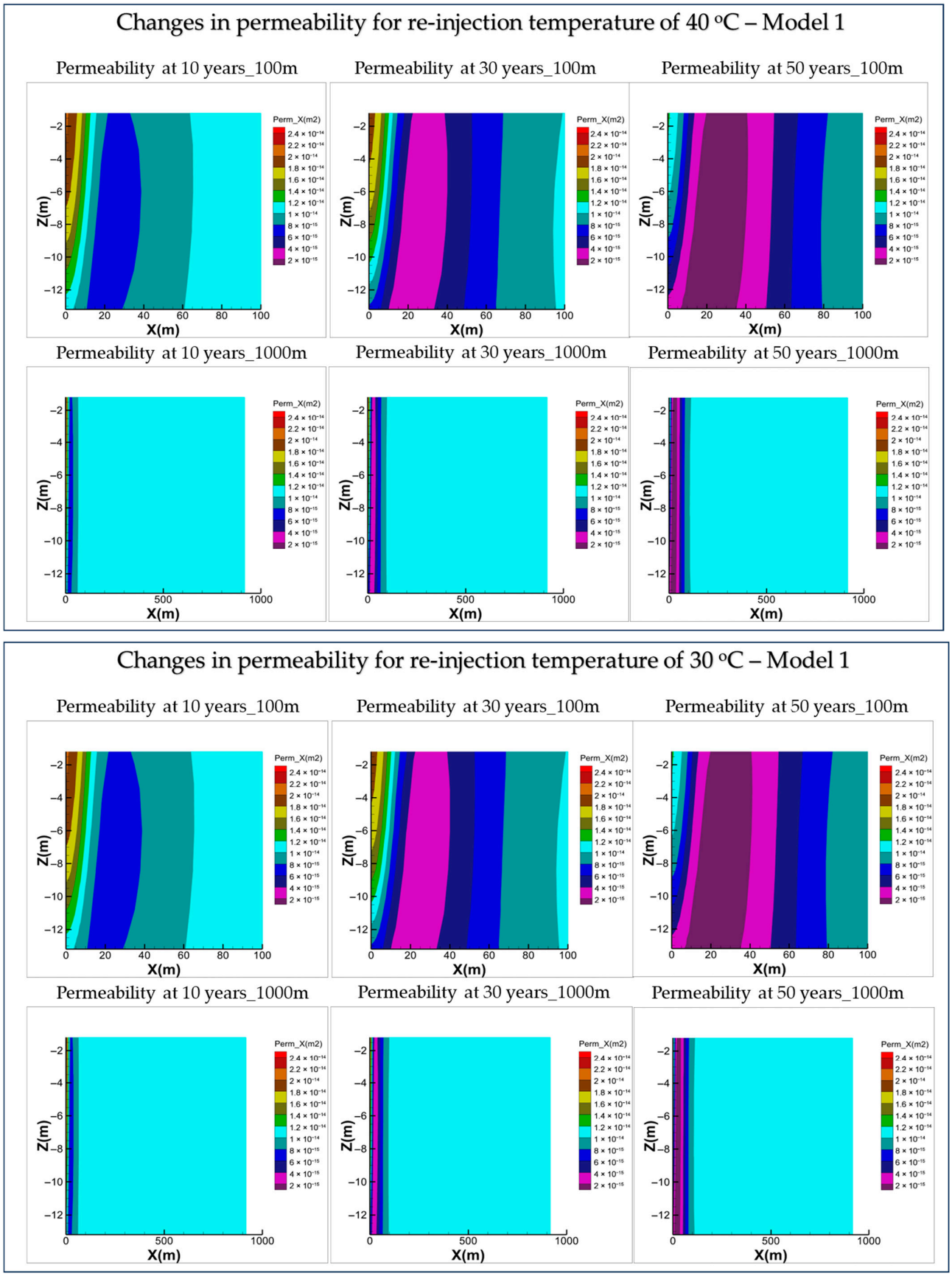

Figure 5. *Cont.*

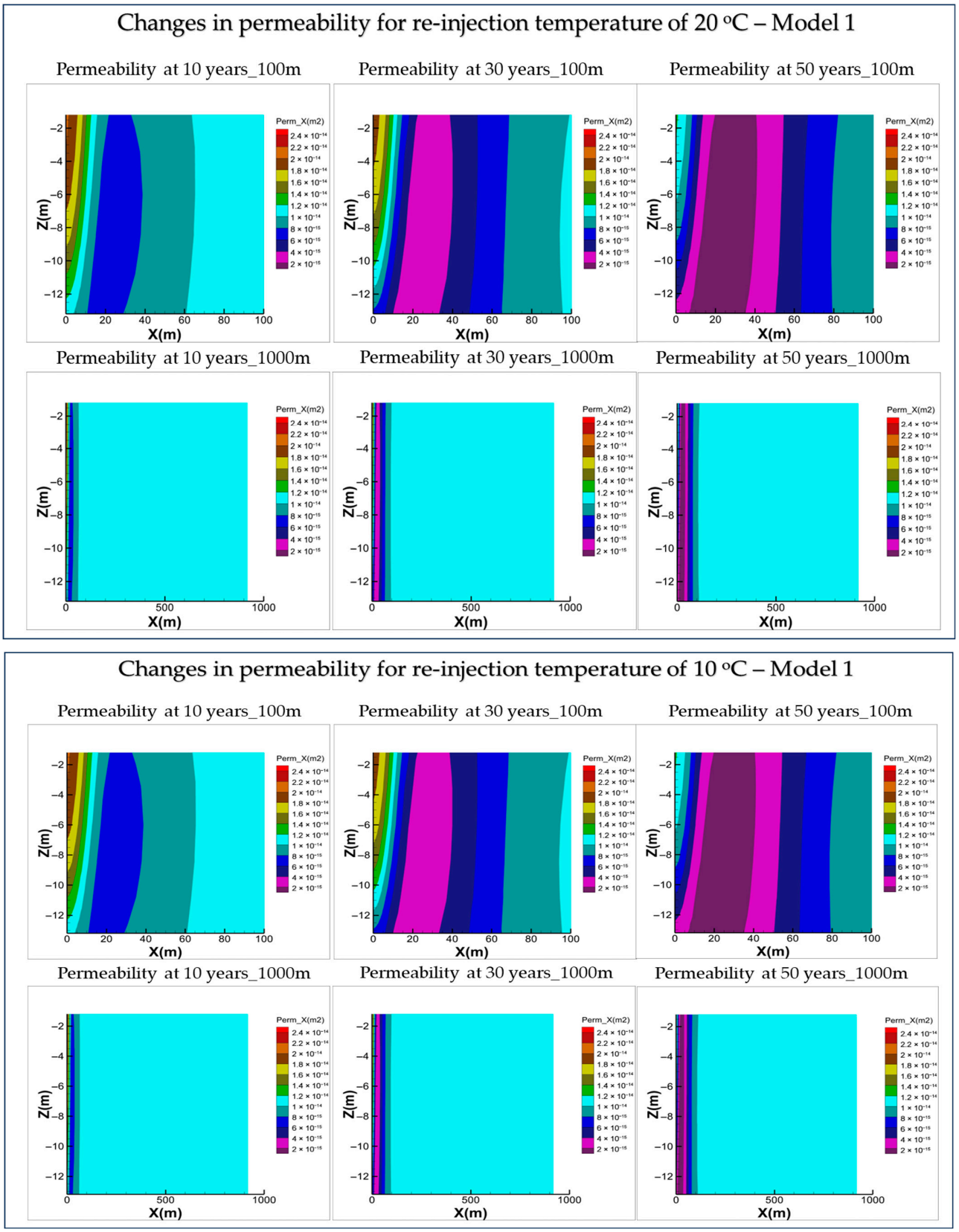

Figure 5. Effect of operation time and injection temperature on reservoir properties–permeability of Model 1, changes shown for reservoir porosity at 100 and 1000 m from injection well. Results are shown for 10, 30, and 50 years.

4.2. Effect of Time and Re-Injection Temperature on Reservoir Properties of Model 2

For Model 2, the initial porosity and permeability are shown in Figures 6 and 7. In Model 2, a hypothetical water injection rate has been considered, and the results from the modeling show that both porosity and permeability increase over time, as the amount of mineral dissolution and precipitation in the reservoir also increases from year 0 to year 50. The porosity near the well increases by 16%, and away from the well (40 m), it decreases by 9%. Meanwhile, permeability near the well increases by 92%, and away from the well (400 m), it decreases by 16%. In addition to that, there is no effect of re-injection temperature on porosity and permeability like Model 1. Moreover, it is also observed that the rate of decrease in permeability in Model 2 is low as compared to Model 1 because the fines have migrated over a large distance in the reservoir, which impairs the reservoir quality due to high water injection rates. Additional figures of Figures 4–7 are provided in the Supplementary Materials.

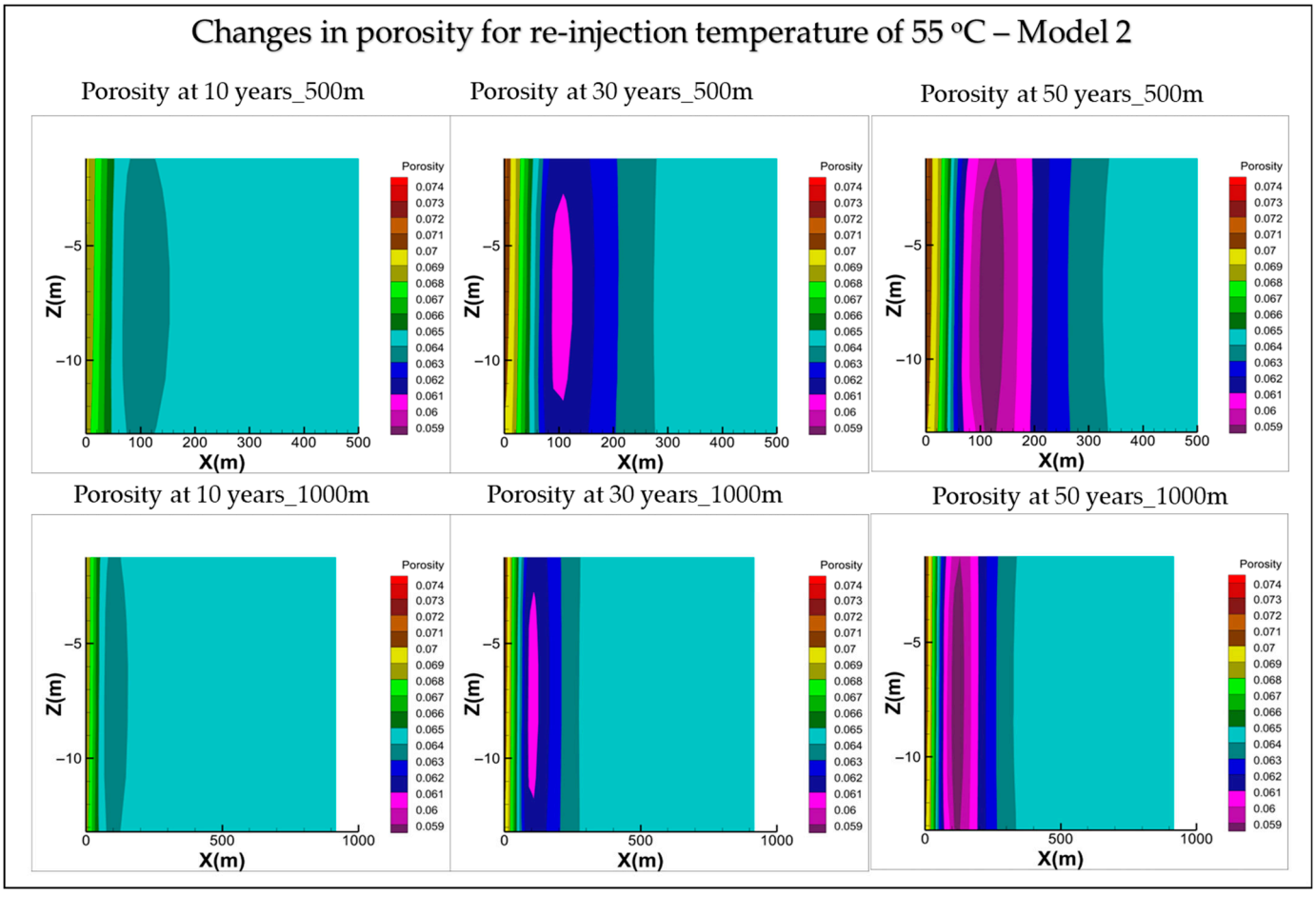

Figure 6. *Cont.*

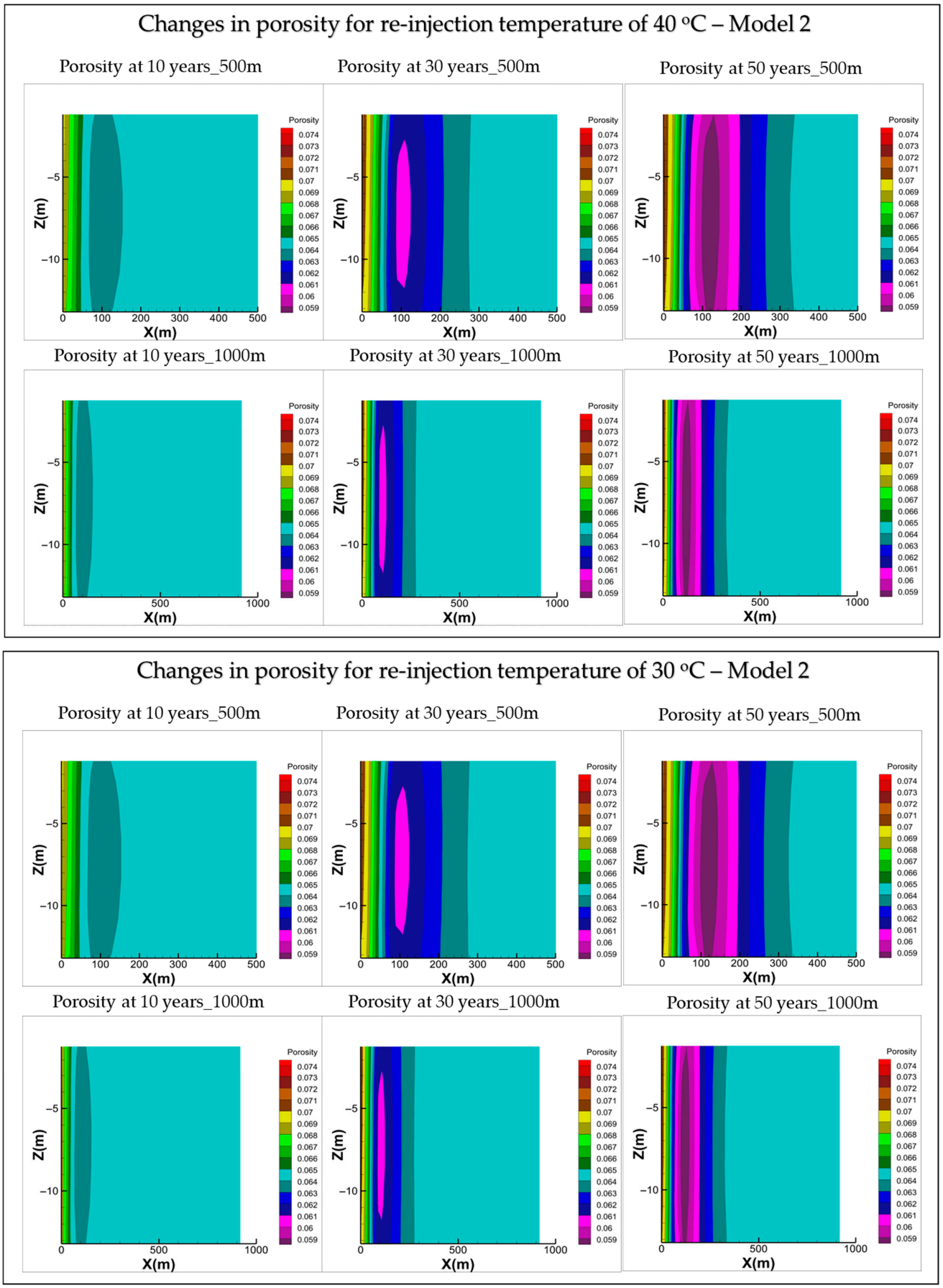

Figure 6. *Cont.*

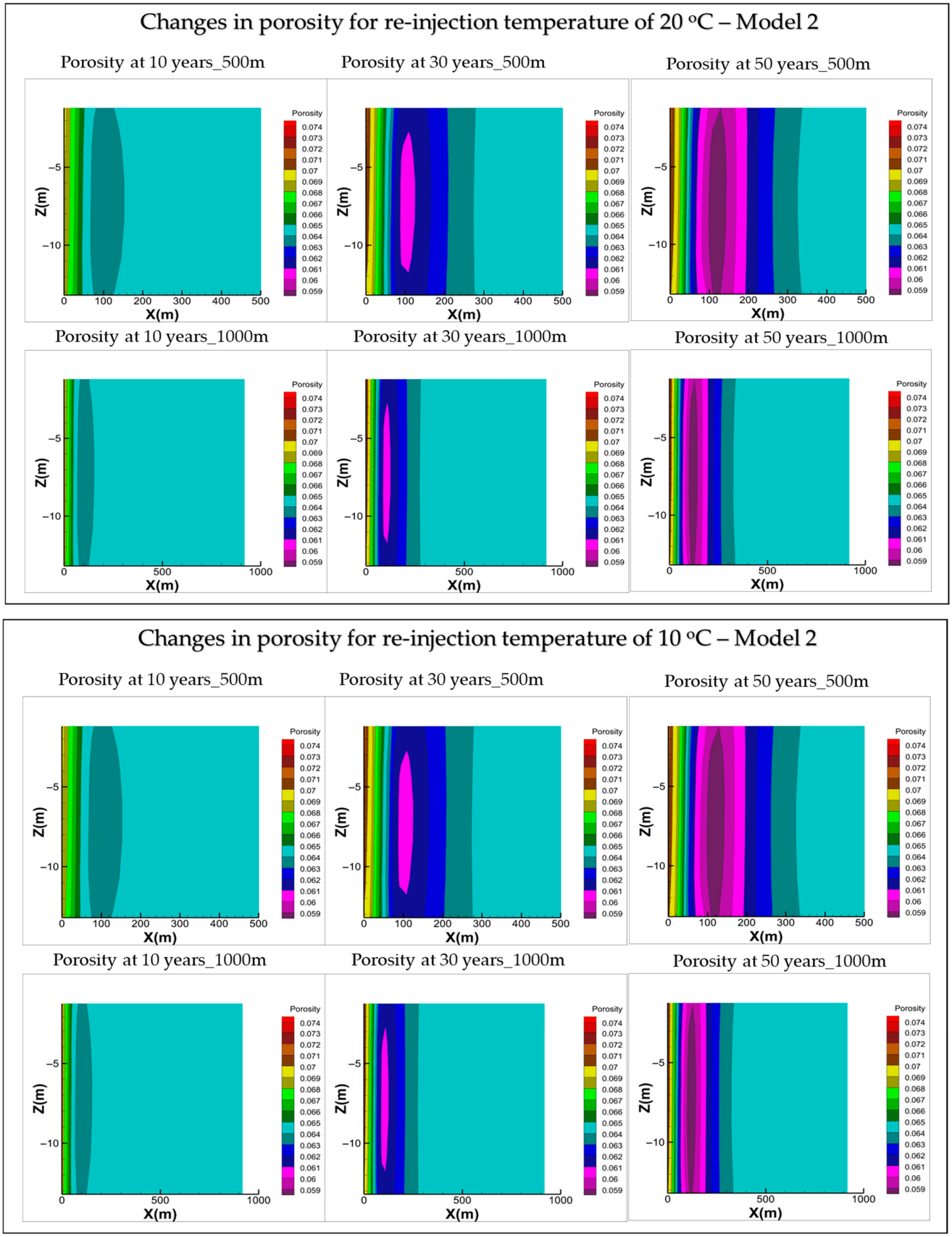

Figure 6. Effect of operation time and injection temperature on reservoir properties–porosity of Model 2, changes shown at 500 m and 1000 m from injection well. Results are shown for 10, 30, and 50 years.

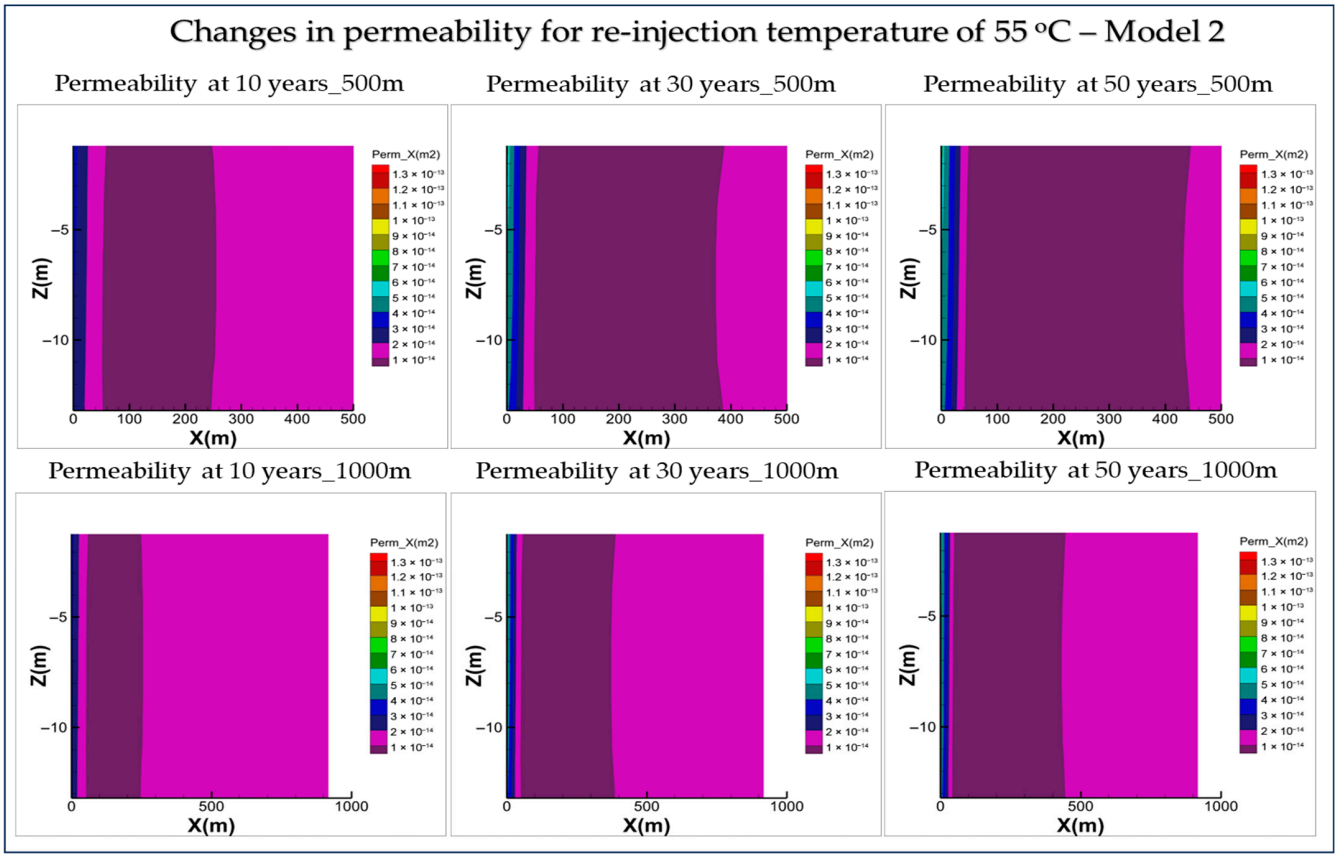

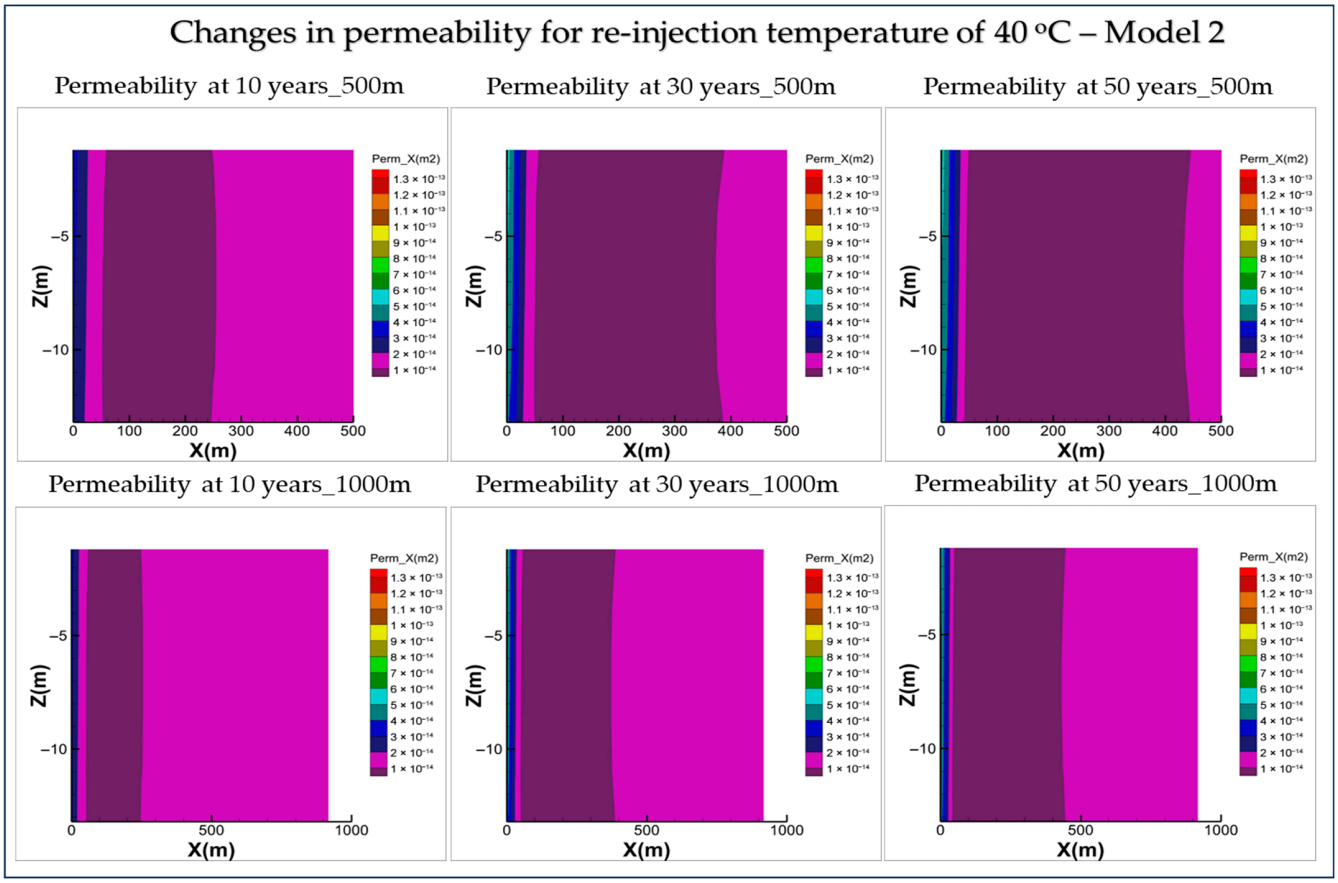

Figure 7. *Cont.*

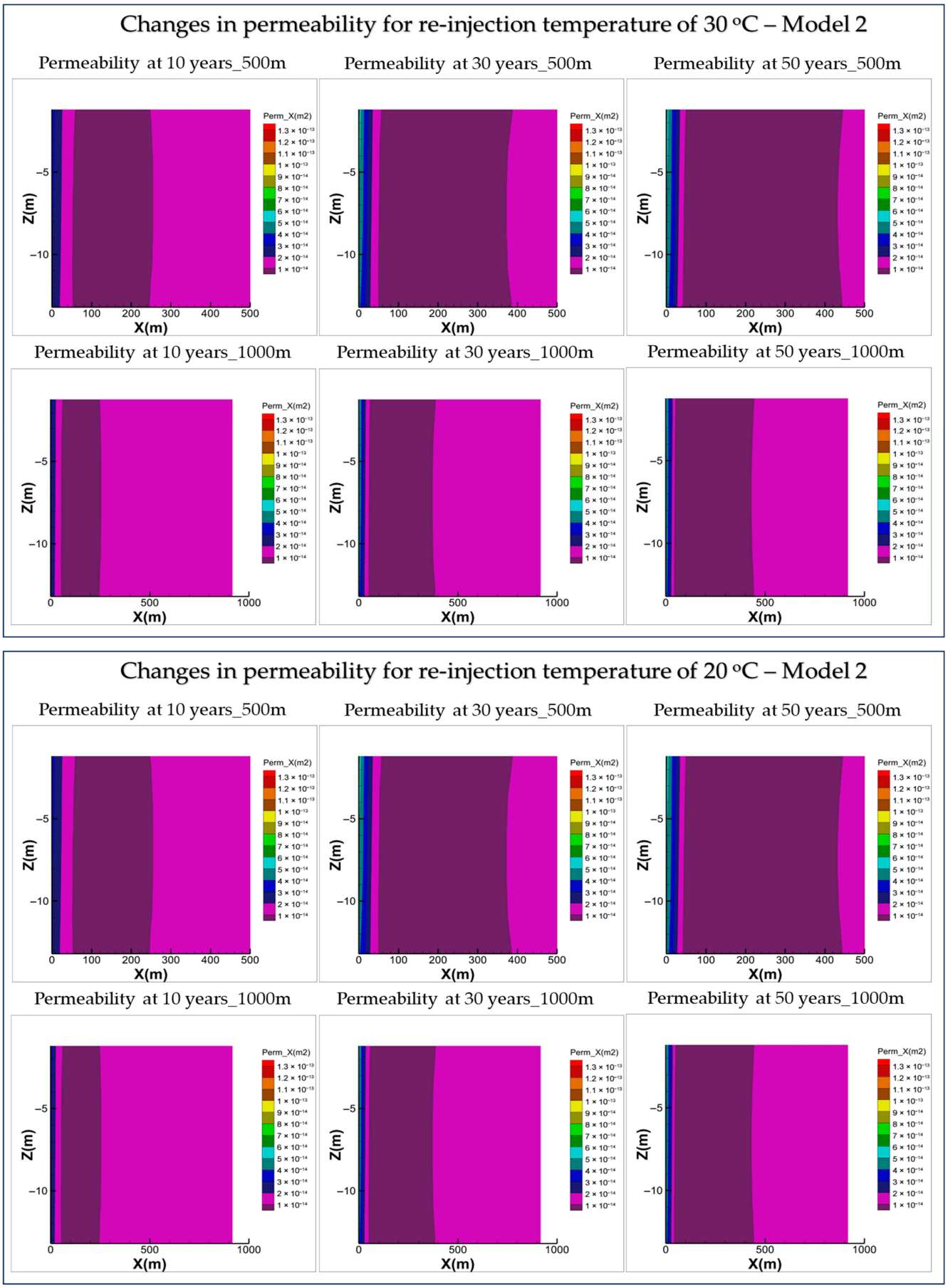

Figure 7. *Cont.*

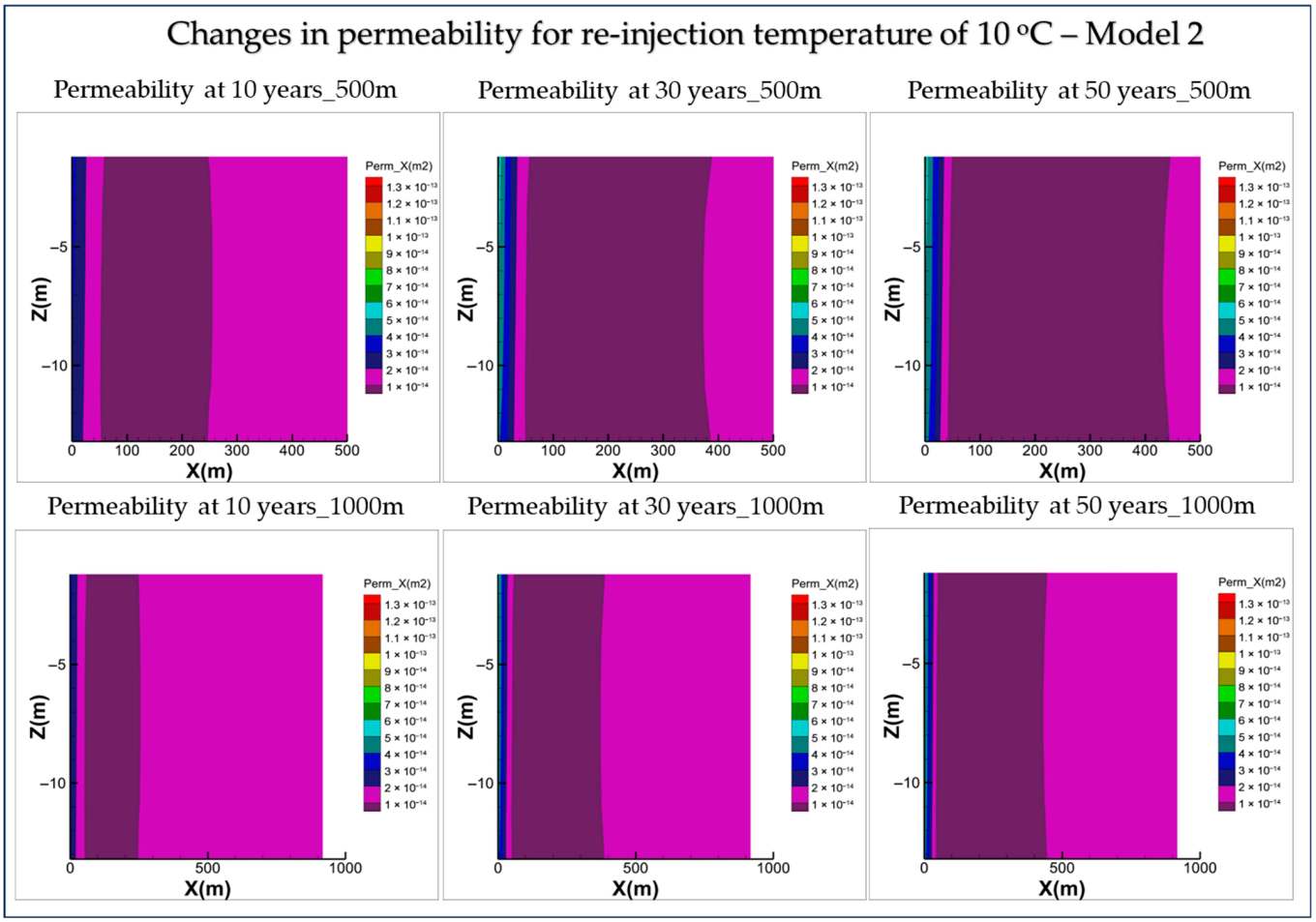

Figure 7. Effect of operation time and injection temperature on reservoir properties–permeability of Model 2, changes shown at 500 m and 1000 m from injection well. Results are shown for 10, 30, and 50 years.

4.3. Mineral Dissolution and Precipitation

Figure 8 shows the temporal evolution of mineral dissolution and precipitation in the Cambrian complex for both Model 1 and Model 2 over 50 years. The improvement in reservoir quality near the well is mainly caused by early-stage mineral dissolution driven by chemical disequilibrium between the injected fluid and the reservoir rock. Illite initially dissolves due to changes in temperature and fluid composition, particularly variations in pH and potassium activity, and later precipitates as the system approaches chemical equilibrium. Anorthite, kaolinite, and dolomite-2 remain in a dissolution phase under the prevailing geochemical conditions. Calcite precipitation is primarily controlled by cooling-induced changes in carbonate equilibrium and CO_2 speciation, while quartz precipitation results from silica supersaturation caused by decreasing temperature. These trends are consistent with the temperature- and chemistry-dependent reaction mechanisms implemented in TOUGHREACT.

From the above-described results, it is concluded that re-injection temperature (from 55 °C to 10 °C) has a negative impact on the reservoir properties. Hence, we conclude that a 40 °C re-injection temperature can be well suited for operating conditions and for power calculations.

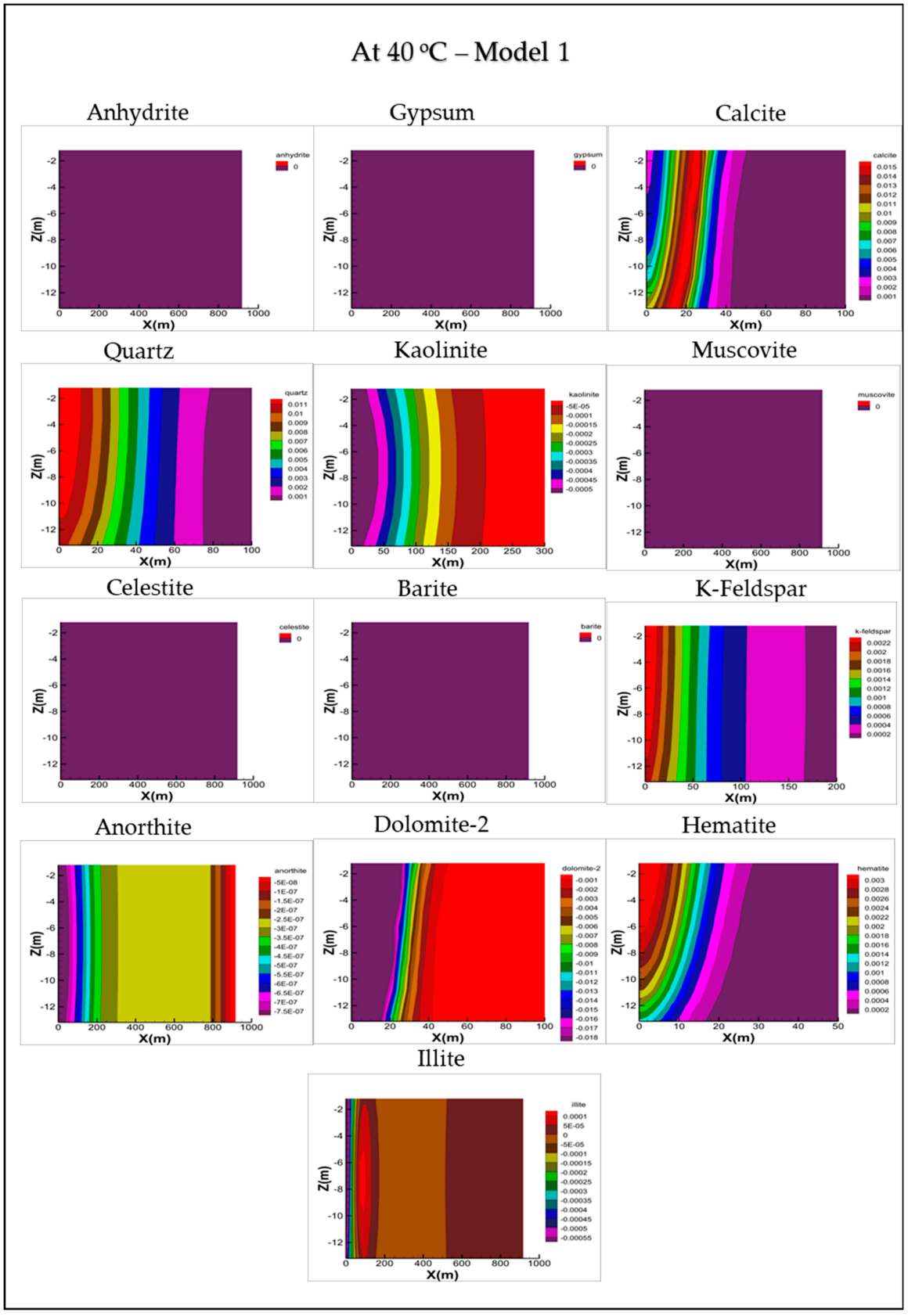

Figure 8. *Cont.*

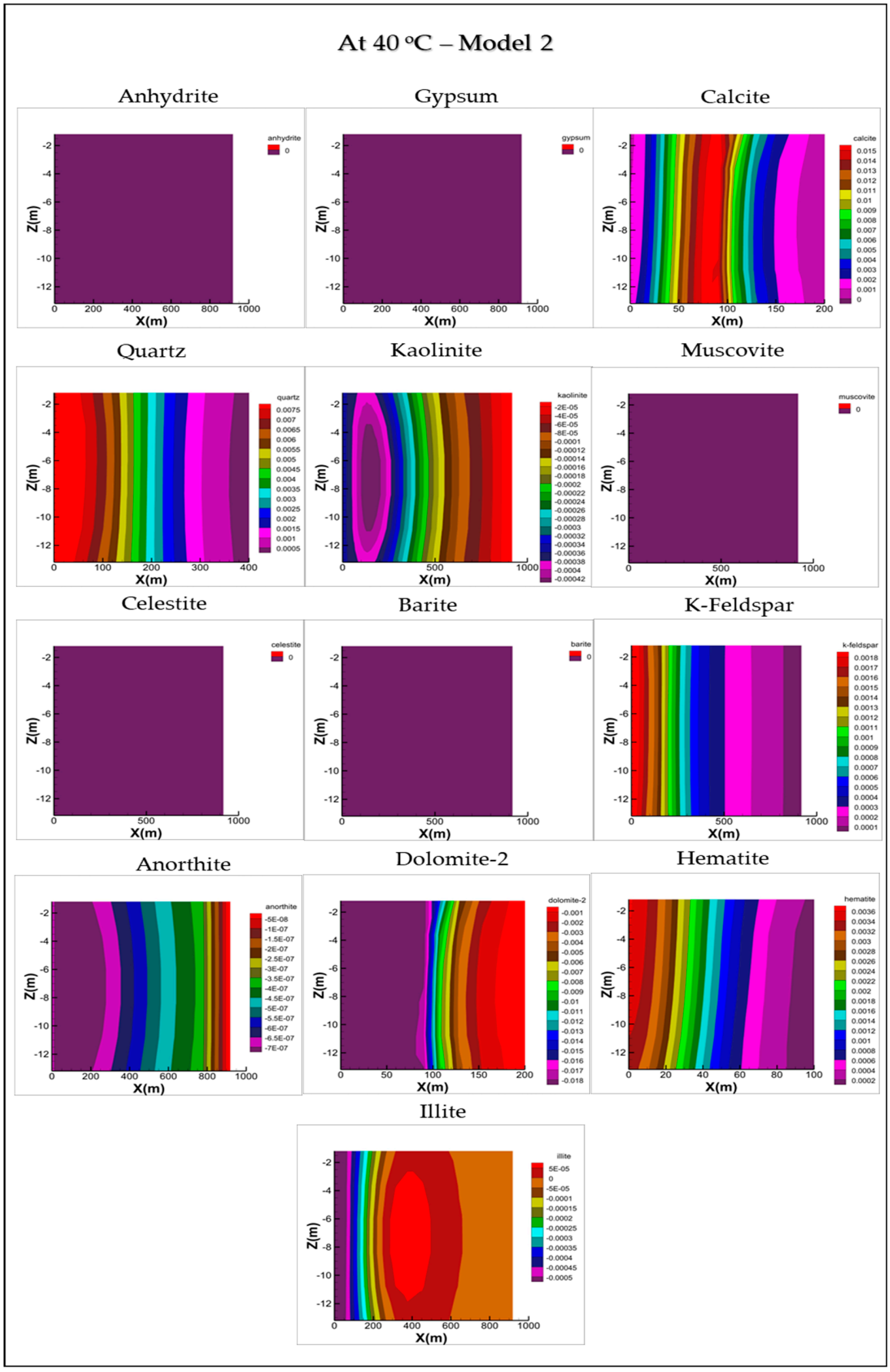

Figure 8. Mineral dissolution (negative values) and mineral precipitation (positive values) at 40 °C, over a 50-year period for both Model 1 and Model 2.

5. Field Development Plan (FDP) of the Screened Cambrian Sites

To prepare the FDP, we have used Multiphysics simulator T-NAVIGATOR (version: v24.3) [24] for modelling and simulation purposes. In our screening study [1], we defined how vertical wells can produce thermal energy (heat) of 37 to 187 GWh. Therefore, in this section, we enhanced the heat energy output by revisiting the field development plan for all of the five screened sites utilizing horizontal wells while considering the re-injection temperature of 40 °C. The preparation of field development plan started with consideration of the mid-case model as the base reference, and both injection and production wells were placed in the water leg, considering different operational scenarios.

5.1. Placement of Horizontal Well

5.1.1. Scenario 1 (Both Injector and Producer at Same Depth)

To find the best spots for horizontal injection and production wells, a long horizontal borehole, 2500 m in length, was drilled in the model. In this setup, both the injector and producer wells were placed at the same depth. Four different locations were tested, as shown in Figure 9. Figure 10 and Table 7 provide details about the well specifications and the average water production and injection rates for mid-case models from all five screened sites.

Table 7. Average water production and injection rate for all screened sites (mid case model).

Horizontal Well Length of 2500 m Long-Depth Sensitivity					
Sr. No	**Reservoirs**	**Depth Z (m)**	**Grid Block**	**Avg. Water Injection Rate (sm^3/day)**	**Avg. Water Production Rate (sm^3/day)**
1	Nausodis	37	53	481.69	604.31
2		50	71	529.26	786.28
3		63	89	428.74	700.26
4		76	107	475.62	751.68
1	Diegliai	24	53	204.48	250.61
2		32	71	219.46	277.14
3		40	89	195.2	328.12
4		48	107	176.37	331.85
1	Vilkyciai	30	53	122.9	182.06
2		40	71	133.88	235.45
3		50	89	112.24	223.15
4		60	107	108.92	208.04
1	Siuparai	13	53	170.93	234.76
2		17	71	174.24	279.06
3		22	89	188.36	257.45
4		26	107	204.18	294.15
1	Genciai	10	53	124.7	219.58
2		14	71	162.71	226.35
3		17	89	92.03	88.53
4		21	107	81.68	185.71

From Table 7, it is found that Nausodis, Vilkyciai, and Genčiai have water production and injection rates higher at a depth of 50 m, 40 m, and 14 m (71 grid blocks), respectively. Meanwhile, Siuparai has the highest water production and injection rates at 26 m (107 grid blocks). Furthermore, Diegliai shows that the highest water injection rate is 32 m (71 grid blocks), and the highest water production rate is 40 m (89 grid blocks), which concludes that there can be an effect of vertical segregation to maximize the water production and injection rates. To observe the vertical segregation effect, we created scenario 2.

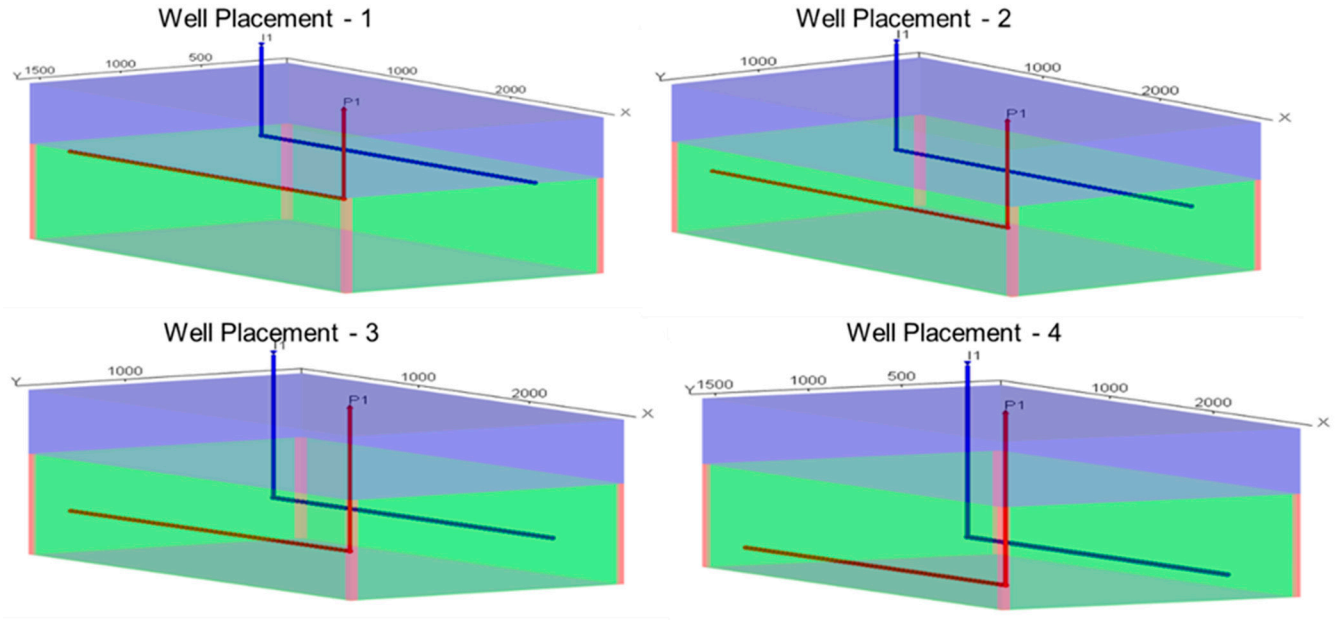

Figure 9. Horizontal Well Placement (Injector (blue) and Producer (red) at same depth) (green box represent aquifer zone).

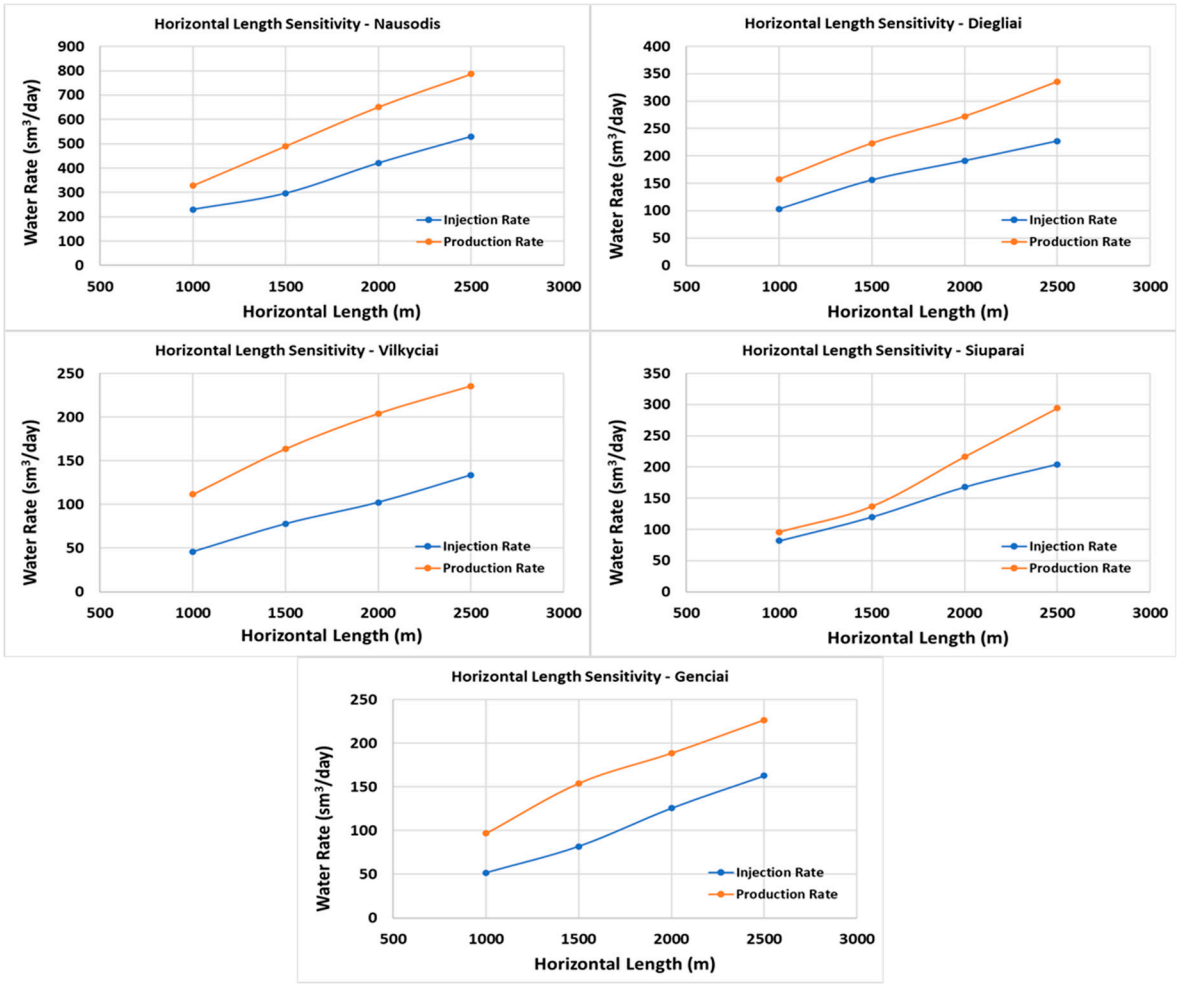

Figure 10. Average water production and injection rate of screened sites (Mid-case model).

5.1.2. Scenario 2 (Lower Injector and Upper Producer)

To maximize the water production and injection rates, we have also analyzed the situation of vertical segregation using horizontal wells. In this setup, the injector is placed below the producer (bottom) and the producer at the top of injector. Like the earlier scenario 1, we have classified three different patterns, as shown in Figure 11. Table 8 provides details about the well specifications and the average water production and injection rates for mid-case models from all five screened sites.

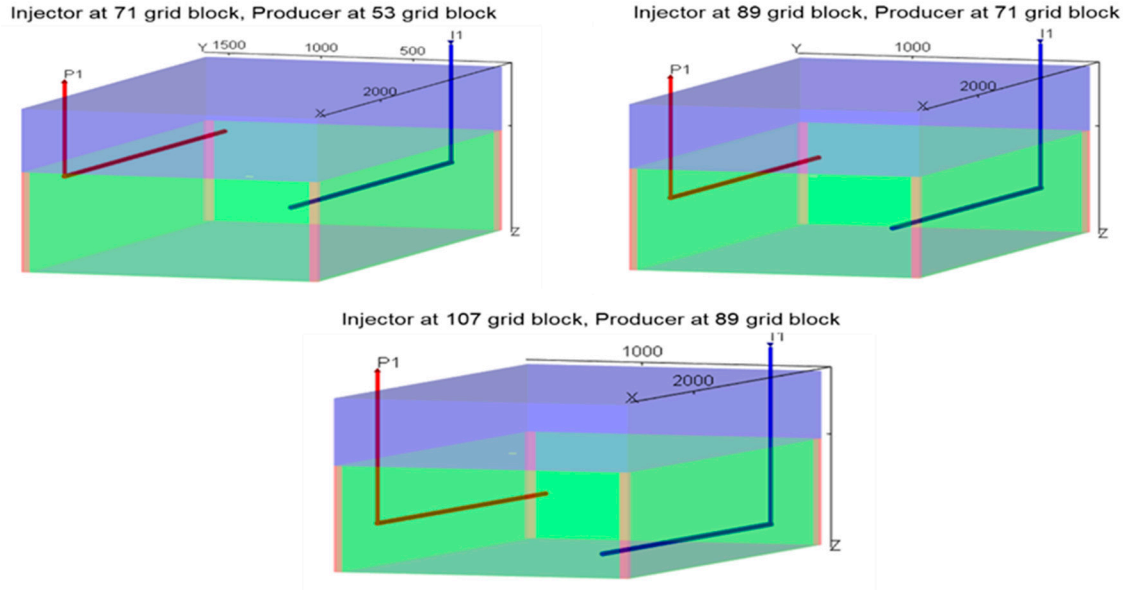

Figure 11. Vertical segregation of horizontal Well (Injector (blue) at bottom and Producer (red) at top)–Scenario 2 (green box represent the aquifer zone).

Table 8. Average water production and injection rate from vertical segregation (Scenario–2).

Vertical Segregation of Horizontal Well-2500 m Long Without Fracturing						
Sr. No	**Reservoirs**	**Depth (m)**		**Length (m)**	**Avg. Water Injection Rate (sm^3/day)**	**Avg. Water Production Rate (sm^3/day)**
		Injector	**Producer**			
1	Nausodis	50	50	2500	529.26	786.28
2		50	37	2500	**489.79**	605.82
3		63	50	2500	438.45	**754.33**
4		76	63	2500	468.17	713.08
1	Diegliai	32	40	2500	227.26	335.46
2		32	24	2500	**216.38**	252.66
3		40	32	2500	188.73	271.28
4		48	40	2500	175.26	**323.33**
1	Vilkyciai	40	40	2500	133.88	235.45
2		40	30	2500	**129.65**	182.81
3		50	40	2500	112.88	**231.87**
4		60	50	2500	109.95	222.85
1	Siupariai	26	26	2500	204.18	294.15
2		17	13	2500	167.32	233.61
3		22	17	2500	192.98	**285.01**
1	Genciai	14	14	2500	162.71	226.35
2		14	10	2500	**163.49**	**232.52**
3		17	14	2500	106.64	208.46
4		21	17	2500	72.09	85.42

From Table 8, it is concluded that there is no substantial effect of vertical segregation on Nausodis and Vilkyciai. Meanwhile, Diegliai still shows that vertical segregation influences the water production rate and water injection rate, which is due to property distribution. For Siupariai, the highest water injection rate is observed at 26 m (107 grid block), while the highest water production rate is 17 m (71 grid block), but that increase is not that substantial as compared to a water production rate of 26 m (107 grid block). Furthermore, Genciai has the highest water production rate of 10 m (53 grid block), which is due to heterogeneous distribution in the model, and the highest water injection rate is observed at 14 m (71 grid block). So, for future study of all screened sites, we have prepared the field development plan as per scenario 1.

5.2. Study of Horizontal Length

The horizontal length of a well is important because longer sections reach more reservoir rock, improving fluid production, recovery efficiency, and overall cost-effectiveness, making better use of the reservoir. Figure 12 depicts the effect of horizontal length on water production and injection rates of all screened sites. From Figure 12, it is observed that water production and injection rates vary linearly with the horizontal length for all the screened sites.

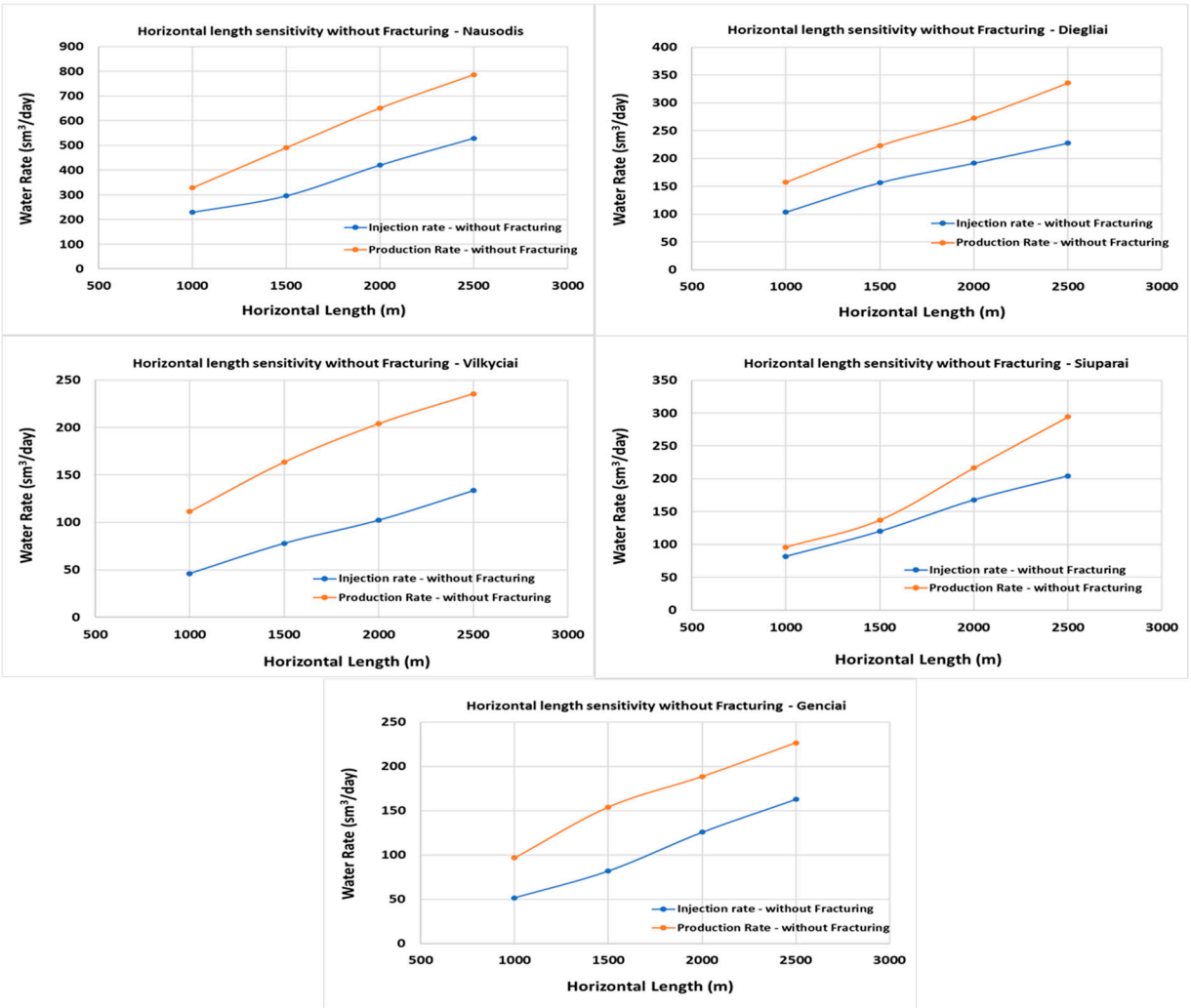

Figure 12. Effect of horizontal length on water production and injection rates (without fracturing–Mid case).

5.3. Enhancing Production and Injection Rates Through Fracturing (500 m Intensity)

Fracturing creates artificial cracks in rocks, helping oil, gas, or water flow into wells. It increases production and allows injection wells to maintain pressure and improve recovery from nearby production wells. Overall, fracturing boosts the efficiency and performance of wells. In our case, to boost the geothermal outputs, we have fractured both the injector and producer. Figure 13 shows the effect of fracturing on water production and injection rates. From Figure 13, it is observed that fracturing elevates the water production and injection rates for all the screened sites and varies linearly with horizontal length.

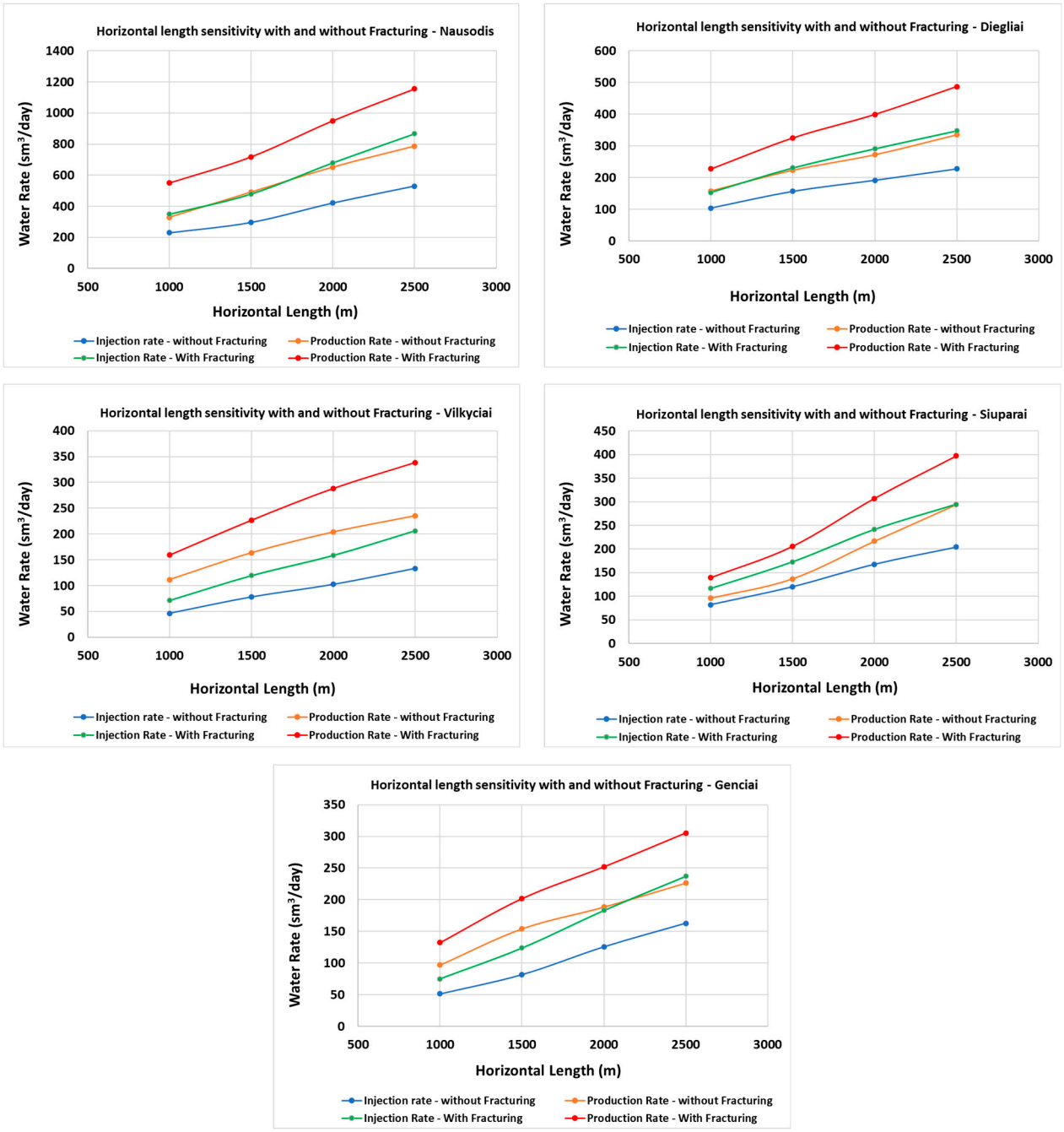

Figure 13. Effect of fracturing on water production and injection rates (Mid-case model).

5.4. Effect of Fracture Intensity for Enhancing Production and Injection Rates

Fracture intensity refers to how many fractures are present and how well they are connected within the reservoir. Higher fracture intensity creates more pathways for fluids

to flow, which can significantly boost production and injection rates. In production wells, more fractures allow oil, gas, or water to reach the wellbore faster and more easily. In injection wells, increased fracture intensity helps injected fluids spread more efficiently into the reservoir, maintaining pressure and improving overall recovery. However, if fracture intensity is too high, it can sometimes cause issues like early water or thermal breakthrough or loss of control over fluid movement. Therefore, optimizing fracture intensity is key to maximizing performance without causing unwanted problems. In our study, we increased the fracture intensity for both producer and injector and limited our intensity rate to 125 m. Figure 14 depicts the effect of fracture intensity on water production and injection rates. Figure 14 concludes that water production and injection rates have an exponential relationship with the fracture intensity for all the screened sites.

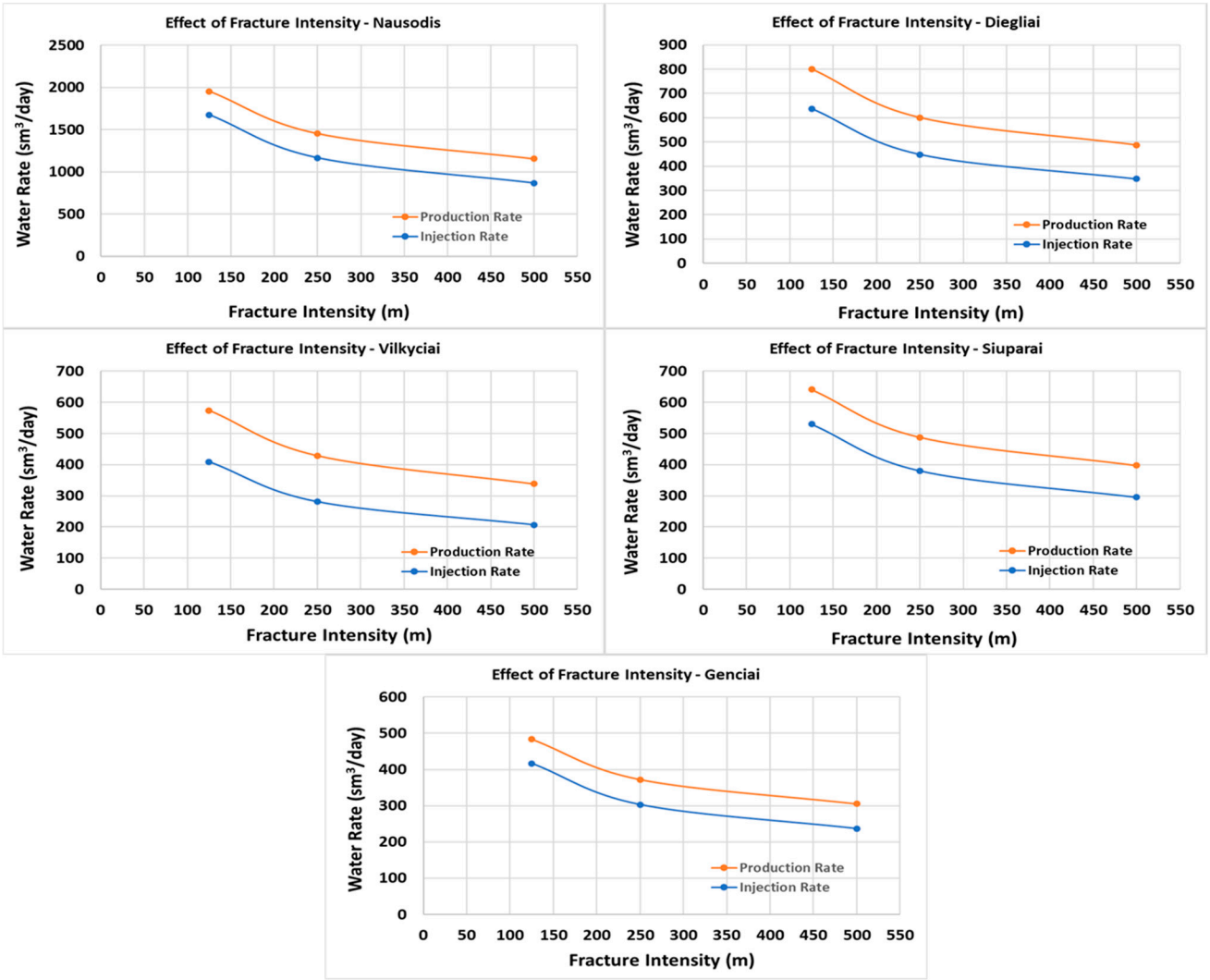

Figure 14. Effect of fracture intensity on water production and injection rates (Mid-case model).

5.5. Comparative Analysis of Low, Mid, and High Cases for Screened Sites

Comparison of low, mid, and high cases for screened sites is important to understand the full range of possible outcomes under different conditions. This comparison helps us in identifying how site performance might vary with changes in various operating conditions and key factors such as flow rates, pressure, or fracture intensity. It also allows for better risk assessment and decision-making by highlighting both the best- and worst-case scenarios. By studying all three cases, we can design more flexible and reliable development strategies, ensuring that the selected sites perform well under a variety of real-world conditions.

Water Production and Injection Rate Without and with Fracturing (500 m Intensity)

Figures 15 and 16 show the comparison of water production and injection rate for low, mid, and high cases for scenarios without and with fracturing for all screened sites. In the low case, both water injection and production rates are 23% lower than in the mid case. In the high case, these rates are 27% higher than in the mid case. Meanwhile, in the case of vertical wells, both water production and injection rates are 10% lower compared to the mid case, while in the high case, these rates are 13% higher than the mid case [1].

Figure 17 shows that increasing fracture intensity gives similar results in the low and high cases. Moreover, the water production and injection rates have an exponential relationship with the fracture intensity. Additionally, none of the cases show thermal breakthrough at the producer during the 50-year simulation, and the temperature front remains within a maximum distance of 700 m from the injector, as shown in Figure 18.

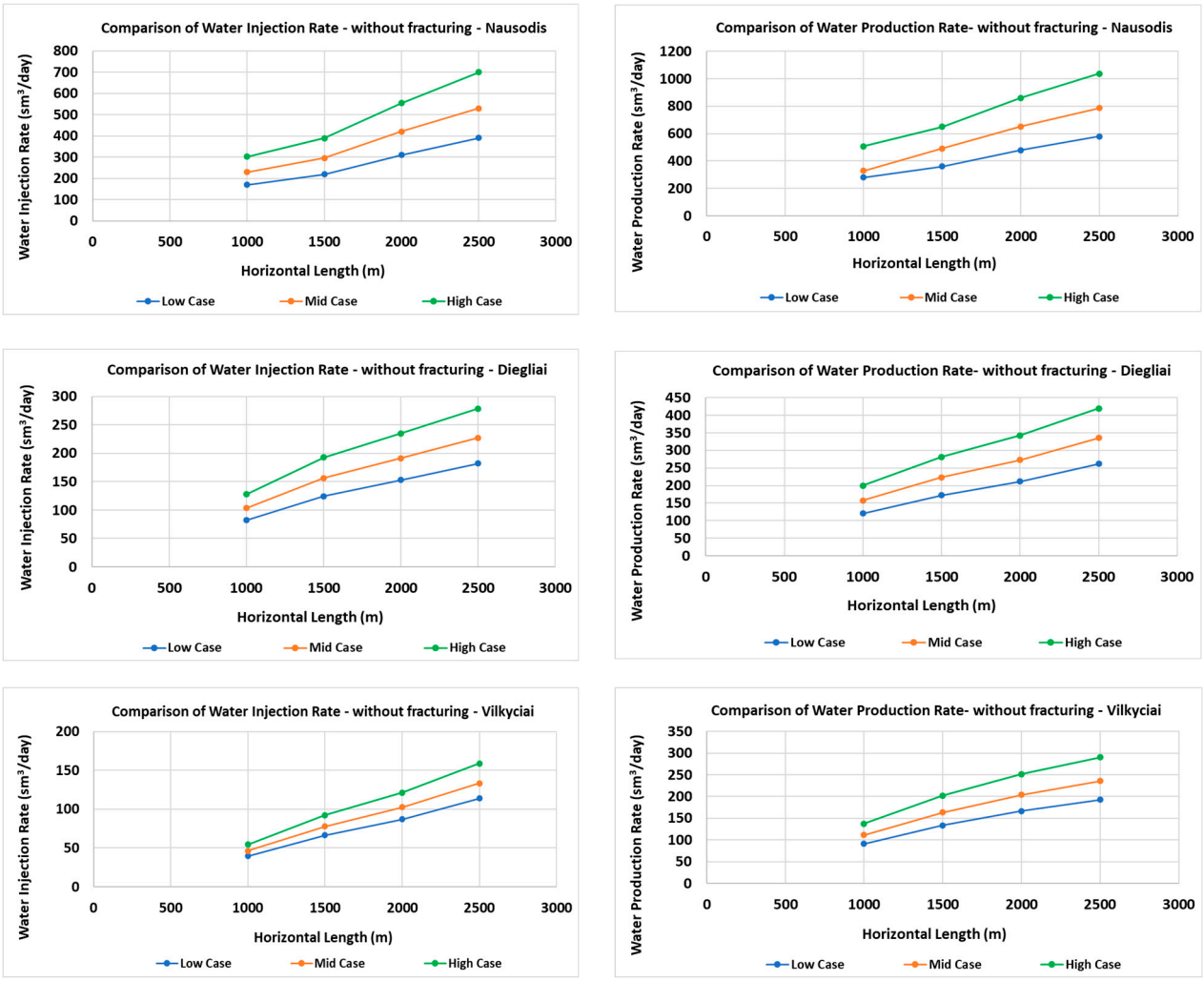

Figure 15. *Cont.*

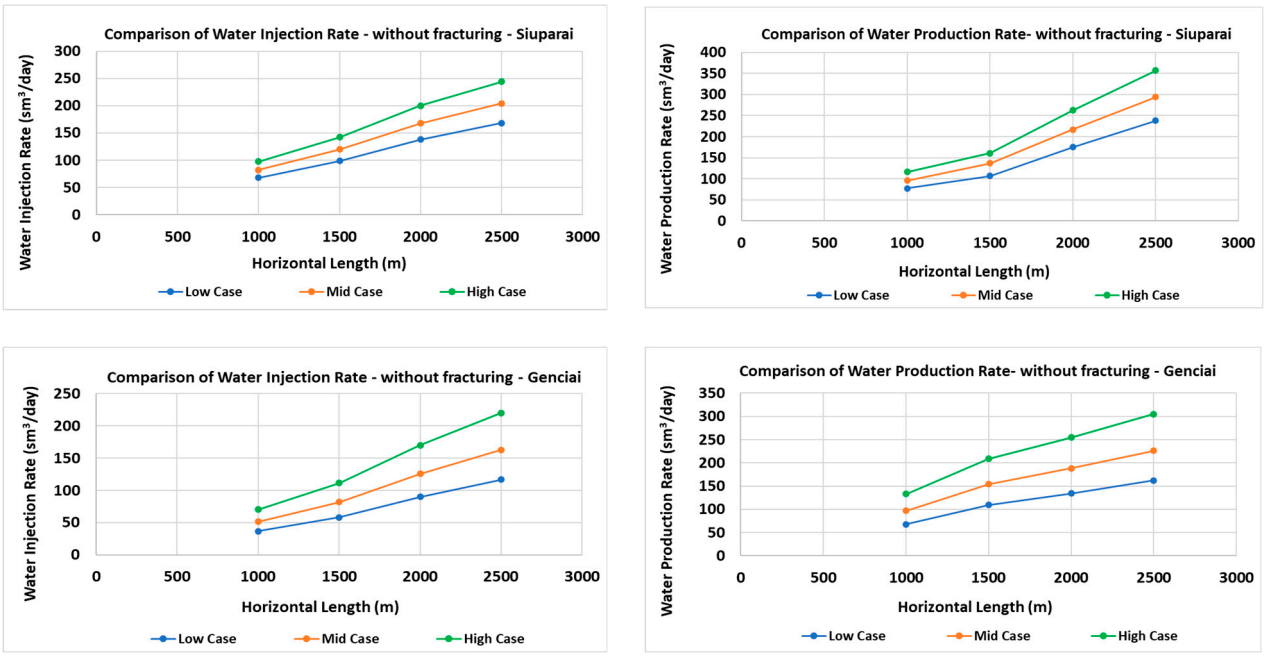

Figure 15. Comparison of low, mid, and high case without fracturing for screened sites.

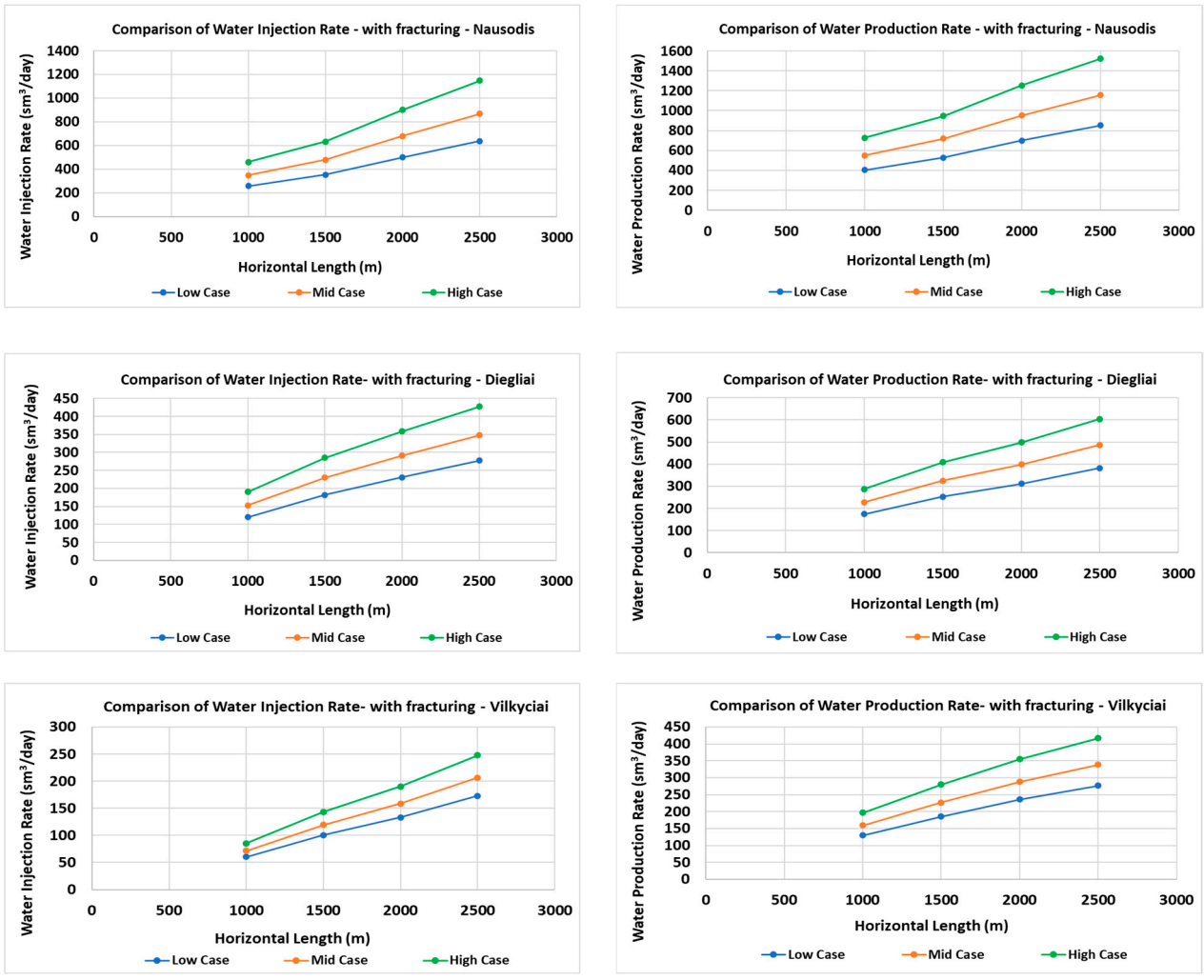

Figure 16. *Cont.*

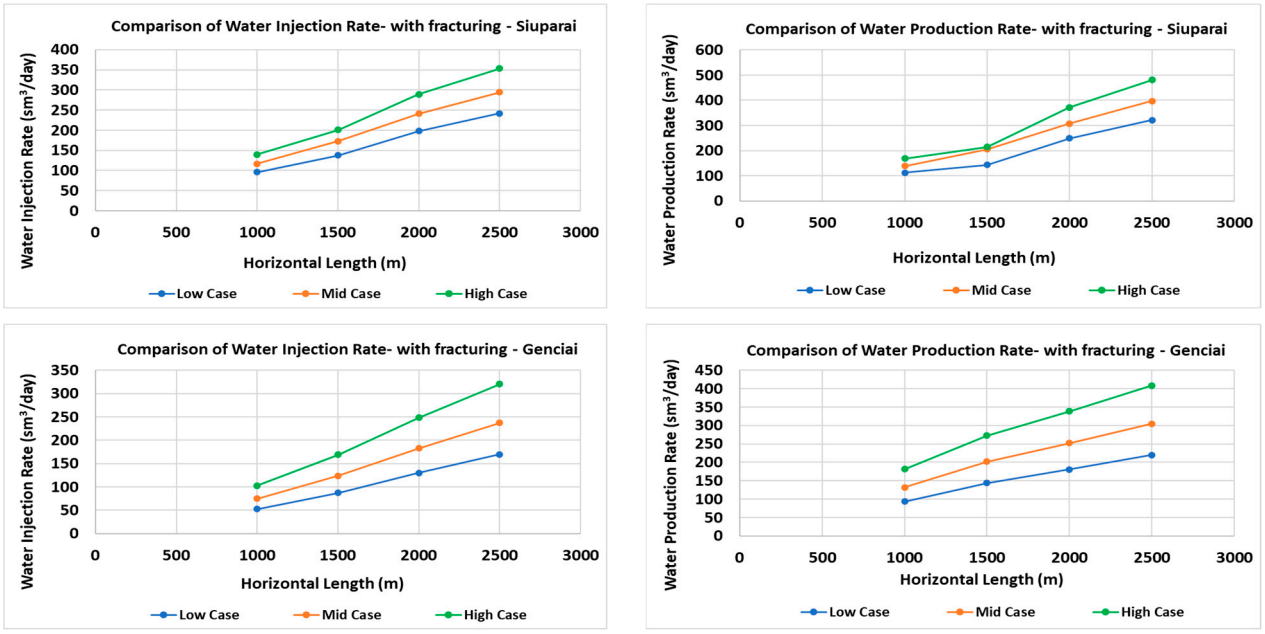

Figure 16. Comparison of low, mid, and high case with fracturing (500 m intensity) for screened sites.

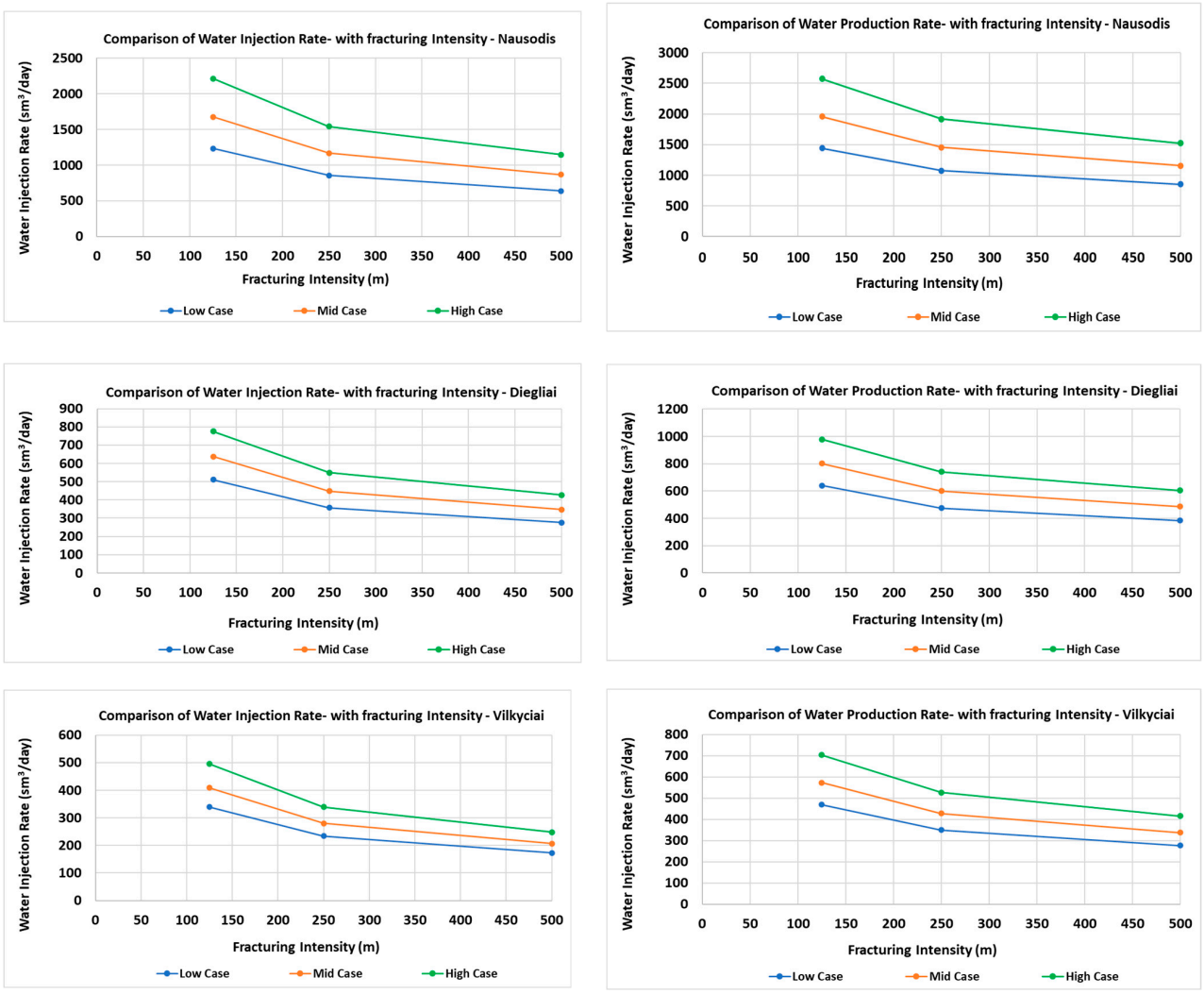

Figure 17. *Cont.*

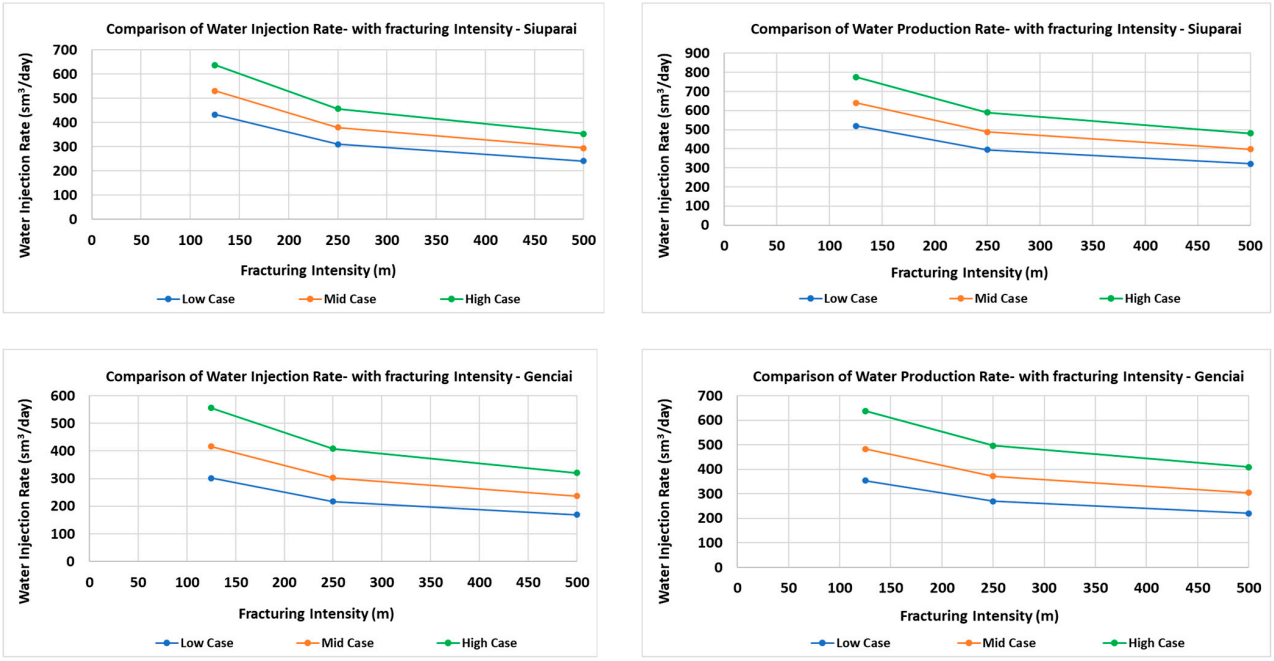

Figure 17. Fracture Intensity comparison of low, mid, and high cases for screened Sites.

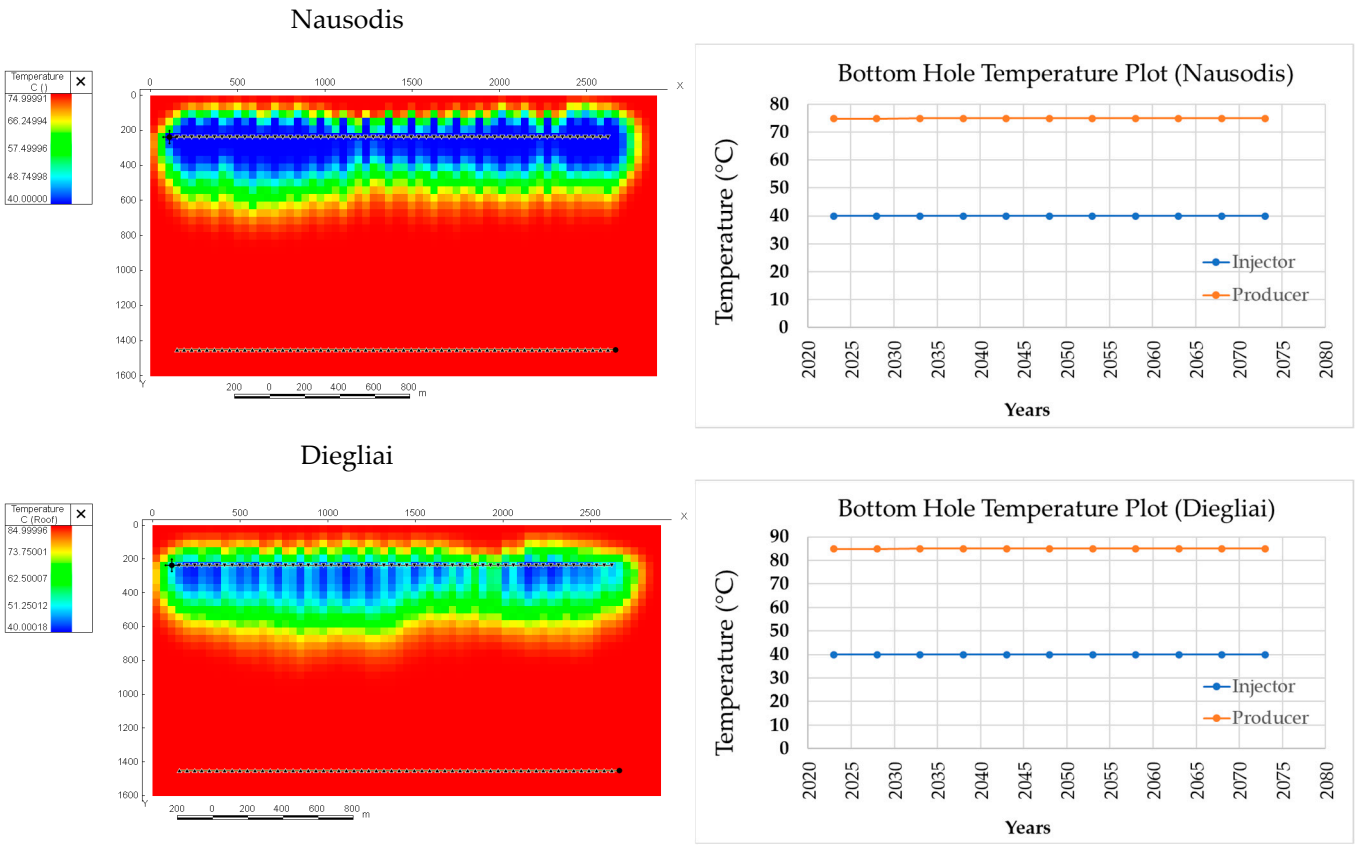

Figure 18. *Cont.*

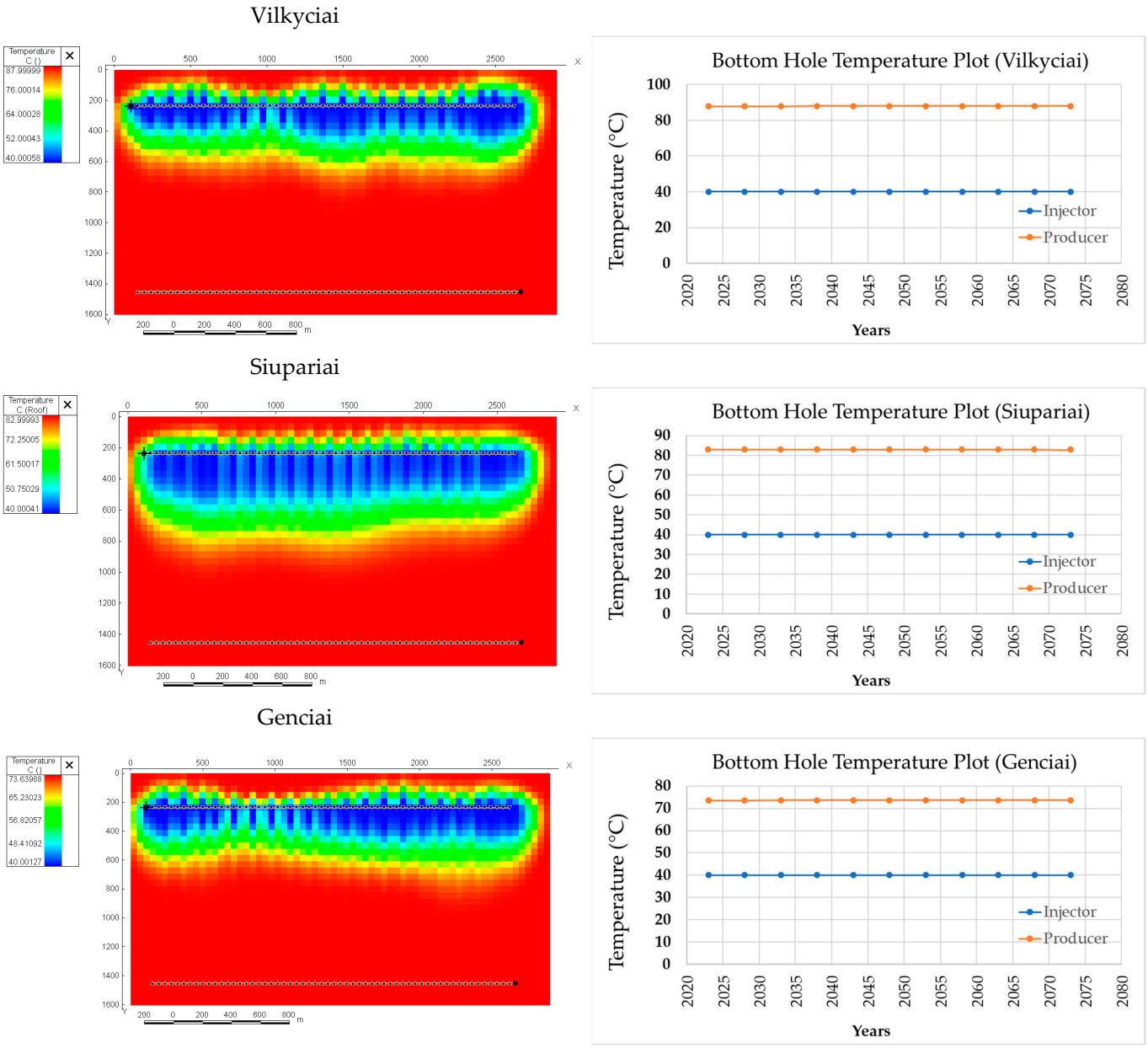

Figure 18. Thermal breakthrough profile of screened sites (High-case model–125 m fracture intensity–50 years).

6. Theoretical Power Assessment of Screened Sites (25 Years History)

Theoretical power assessment is a critical step in the development of geothermal energy projects. Meanwhile, design power assessment determines how the power plant can be operated to minimize the loss of power. Thus, both involve estimating the amount of energy that can be sustainably extracted from a geothermal reservoir over time. This assessment helps determine the technical and economic viability of the project by providing essential data on expected power output. It supports the design and sizing of geothermal plants, informs investment decisions, and helps minimize risks associated with uncertain subsurface conditions. Furthermore, a reliable power assessment is often required by regulatory authorities and financial institutions before granting permits or funding. Overall, power assessment lays the foundation for the successful planning, development, and operation of geothermal energy systems. Thus, in this study, we compare the theoretical

power that can be extracted from the given site over time using theoretical equations, which are described as follows.

$$Q = m \times Cp \times \Delta T \quad (1)$$

$$Pth = Q/t \quad (2)$$

where Q is the Energy (heat flow in Watts), m is mass flow rate kg/h with density of water 1129 kg/m^3, Cp is the specific heat of water is 4200 J/kg·°K, and ΔT is the temperature difference and Power (Pth) in KW, with t as time in hours.

To compare power output results, we present the example of the Vilkyčiai reservoir. In our earlier study [1], the high-case model showed that a vertical well could produce 242 m^3/day of water, generating 0.44 MW of power with a temperature difference of 33 °C. In our subsequent study [3], we increased water production by using horizontal wells. The mid-case model with horizontal wells produced 339 m^3/day of water—a 40% increase—resulting in 0.61 MW of power, a 38% increase, while maintaining the same temperature difference of 33 °C. In the present study, we further enhanced power output by lowering the reinjection temperature to 40 °C, achieving a temperature difference of 48 °C. This resulted in a power (thermal) output of 0.89 MW, a 46% increase compared to the study [3]. Thus, the resulting enhanced power outputs from all screened sites are summarized in Table 9.

Table 9. Power (Thermal) calculation for the screened sites using horizontal wells.

Horizontal Well Length (2500 m Long)—With Fracturing Sensitivity-25 Years								
Sr. No	**Reservoirs**	**Fracture Intensity (m)**	**Case**	**Avg. Water Injection Rate (sm^3/day)**	**Avg. Water Production Rate (sm^3/day)**	**Heat Energy (W)**	**Heat Energy (GWh)**	**Power (MWth)**
1	Nausodis	125	Low	1232.59	1442.77	2.187×10^{15}	607.36	2.77
			Mid	1676.1	1955.71	2.964×10^{15}	823.29	3.76
			High	2212.37	2574.46	3.902×10^{15}	1083.77	4.95
2		250	Low	857.25	1073.07	1.626×10^{15}	451.73	2.06
			Mid	1166.59	1454.96	2.205×10^{15}	612.49	2.80
			High	1541.84	1916.16	2.904×10^{15}	806.65	3.68
3		500	Low	637.83	851.96	1.291×10^{15}	358.65	1.64
			Mid	867.69	1155.33	1.751×10^{15}	486.36	2.22
			High	1147.38	1521.98	2.307×10^{15}	640.71	2.93
1	Diegliai	125	Low	511.19	639.23	1.246×10^{15}	345.98	1.58
			Mid	637.34	800.36	1.559×10^{15}	433.19	1.98
			High	776.02	978.41	1.906×10^{15}	529.56	2.42
2		250	Low	357.68	474.21	9.240×10^{14}	256.66	1.17
			Mid	448.63	599.87	1.169×10^{15}	324.68	1.48
			High	550.04	740.57	1.443×10^{15}	400.83	1.83
3		500	Low	276.93	382.63	7.456×10^{14}	207.10	0.95
			Mid	347.58	486.79	9.485×10^{14}	263.47	1.20
			High	426.8	604.14	1.177×10^{15}	326.99	1.49
1	Vilkyciai	125	Low	339.34	469.22	9.752×10^{14}	270.89	1.24
			Mid	408.8	573.6	1.192×10^{15}	331.16	1.51
			High	495.84	704.28	1.464×10^{15}	406.60	1.86
2		250	Low	233.81	350.45	7.284×10^{14}	202.33	0.92
			Mid	280.43	428.69	8.910×10^{14}	247.50	1.13
			High	339.08	527.17	1.096×10^{15}	304.35	1.39
3		500	Low	173.02	276.64	5.750×10^{14}	159.71	0.73
			Mid	206.22	338.42	7.034×10^{14}	195.38	0.89
			High	247.82	416.4	8.654×10^{14}	240.40	1.10

Table 9. *Cont.*

Horizontal Well Length (2500 m Long)—With Fracturing Sensitivity-25 Years								
1	Siupariai	125	Low	432.68	519.69	9.676×10^{14}	268.78	1.23
			Mid	530.29	640.97	1.193×10^{15}	331.50	1.51
			High	637.51	775.14	1.443×10^{15}	400.90	1.83
2		250	Low	310.76	395.22	7.359×10^{14}	204.40	0.93
			Mid	380.08	487.88	9.084×10^{14}	252.33	1.15
			High	456.33	590.56	1.100×10^{15}	305.43	1.39
3		500	Low	241.6	321.79	5.991×10^{14}	166.43	0.76
			Mid	294.76	397.37	7.399×10^{14}	205.52	0.94
			High	353.41	481.33	8.962×10^{14}	248.94	1.14
1	Genciai	125	Low	301.36	353.71	5.152×10^{14}	143.12	0.65
			Mid	416.5	483.26	7.039×10^{14}	195.53	0.89
			High	556	638.29	9.297×10^{14}	258.26	1.18
2		250	Low	217.35	269.88	3.931×10^{14}	109.20	0.50
			Mid	303.11	372.3	5.423×10^{14}	150.64	0.69
			High	408.45	496.2	7.228×10^{14}	200.77	0.92
3		500	Low	169.5	219.99	3.204×10^{14}	89.01	0.41
			Mid	237.05	305.15	4.445×10^{14}	123.47	0.56
			High	320.52	408.75	5.954×10^{14}	165.39	0.76

From Table 9, based on the mid-case evaluation, it is concluded that, among the sites, Nausodis has the highest power output. This is because it has a very high production rate. Diegliai stands second because of production rate as compared to the remaining sites. Vilkyciai and Siupariai have almost similar thermal outputs because they share similar geological properties. Genciai ranks fifth, with lower power potential due to its lower reservoir temperature and poor production rate.

7. Discussion

This study highlights the importance of enhanced water and power production using an uncertainty-modelling workflow published in earlier studies [1–3,23] to evaluate the geothermal potential of depleted hydrocarbon reservoirs. The study demonstrates that horizontal wells can increase water production and injection rates, which leads to higher power output from potential geothermal development sites in Lithuania.

A mechanistic model was used to develop the Field Development Plan (FDP) for the selected sites. In the reservoir model, the maximum horizontal well length is limited to 2500 m. This limitation was addressed by studying the effect of horizontal well length on water production and injection rates, and the observed relationship is linear, using the same well spacing of 1200 m, consistent with previous studies [1–3,23].

The maximum fracture intensity that can be included in the simulation model is 125 m. This limitation was addressed by analyzing the effect of fracture intensity on water production and injection rates. An exponential relationship was observed, indicating a strong influence of fracture intensity on these rates. The study also shows that vertical segregation has a minimal effect, while reservoir heterogeneity has a significant impact.

8. Conclusions

To study the geochemical effect on the screened sites of Lithuania, a reactive transport model has been developed. Re-injection temperature ranges of 10 °C to 55 °C were assumed. The reactive transport modelling shows that there is an effect of mineral dissolution and precipitation within the reservoir. It also shows that mineral dissolution and precipitation are not affected by re-injection temperature from 55 °C to 10 °C, but they are result of the injection pressure rate. Modelling work also shows that 40 °C re-injection temperature

could be applicable for the field development plan for all screened sites and can help to maximize the power output while minimizing reservoir cooling over time.

Modelling work also shows that the horizontal wells have better efficiency compared to vertical wells in terms of operation and reservoir exposure. The application of horizontal wells not only maximizes the water production but also enhances the power (thermal) output by having a linear relationship between the water production and injection rates. Furthermore, fracturing to increase the permeability also enhances the water production and injection rate. In addition to that, increasing the temperature differential between production and reinjection points (e.g., from 33 °C to 48 °C–Vilkyciai reservoir) led to a significant increase in power output. Nausodis is ranked first, followed by Diegliai on second position, followed by Siupariai and Vilkyciai. Genciai further acquires fifth place because of low reservoir properties and temperature.

Thus, this study underpins, overall, the above integrated approach to support the optimized development of geothermal resources in Lithuania. While thermal, hydraulic, and geochemical analyses help to evaluate the performance of geothermal systems under various operating scenarios, they are constrained by site-specific geological characteristics that greatly influence production potential.

Supplementary Materials: The following supporting information can be downloaded at: https://www.mdpi.com/article/10.3390/pr14020203/s1, Figure S1: Effect of operation time and injection temperature on reservoir properties–porosity of Model 1; Figure S2: Effect of operation time and injection temperature on reservoir properties–permeability of Model 1; Figure S3: Effect of operation time and injection temperature on reservoir properties, porosity, of Model 2; Figure S4: Effect of operation time and injection temperature on reservoir properties, permeability, of Model 2.

Author Contributions: Conceptualization, A.R.A.N.M. and M.P.; Methodology, A.R.A.N.M. and M.P.; Software, A.R.A.N.M. and M.P.; Validation, A.R.A.N.M. and M.P.; Formal analysis, A.R.A.N.M. and M.P.; Investigation, A.R.A.N.M. and M.P.; Resources, M.P.; Data curation, A.R.A.N.M. and M.P.; Writing—original draft, A.R.A.N.M. and M.P.; Writing—review & editing, A.R.A.N.M. and M.P.; Visualization, A.R.A.N.M. and M.P.; Supervision, M.P.; Project administration, M.P.; Funding acquisition, M.P. All authors contributed equally. All authors have read and agreed to the published version of the manuscript.

Funding: This project has received funding from the Research Council of Lithuania (LMT), Agreement No. P-MIP-23-102.

Data Availability Statement: The original contributions presented in this study are included in the article/Supplementary Materials. Further inquiries can be directed to the corresponding author.

Acknowledgments: The authors would express their thanks for the LMT funding from Project No. P-MIP-23-102 for supporting the research work presented in this paper. The authors would also like to thank Klaipeda Energy and Minijos Nafta for the subsurface insights during this work. The authors would like to acknowledge support from Rock and Fluids Lab IIT Roorkee, TU Delft, and Innargi A/S. Also, support from software provider Rock Flow Dynamics (Houston, TX, USA) for T-navigator is greatly appreciated. The authors would also like to acknowledge the support from Pijus Makauskas and Ieva Kaminskaite-Baranauskiene for their valuable contributions during the development of the models and reactive transport modelling.

Conflicts of Interest: The authors declare no conflicts of interest.

References

1. Makauskas, P.; Kaminskaite-Baranauskiene, I.; Rashid Abdul Nabi Memon, A.; Pal, M. Assessing Geothermal Energy Production Potential of Cambrian Geothermal Complexes in Lithuania. *Energies* **2024**, *17*, 1054. [CrossRef]
2. Memon, A.R.; Makauskas, P.; Kaminskaite-Baranauskiene, I.; Pal, M. Unlocking Geothermal Energy: A Thorough Literature Review of Lithuanian Geothermal Complexes and Their Production Potential. *Energies* **2024**, *17*, 1576. [CrossRef]

3. Memon, A.R.A.N.; Makauskas, P.; Kaminskaite-Baranauskiene, I.; Pal, M. Workflow for Assessing Geothermal Potential of Depleted Hydrocarbon Fields: A Study of Cambrian Reservoirs in Lithuania. In *Proceedings of the European Association of Geoscientists & Engineers, Oslo, Norway, 2–5 September 2024*; ECMOR: Oslo, Norway, 2024; pp. 1–13. [CrossRef]
4. Zajacs, A.; Shogenova, A.; Shogenov, K.; Volkova, A.; Sliaupa, S.; Sliaupiene, R.; Jõeleht, A. Utilization of geothermal energy: New possibilities for district heating networks in the Baltic states. *Renew. Energy* **2025**, *242*, 122375. [CrossRef]
5. Brehme, M.; Blöcher, G.; Regenspurg, S.; Milsch, H.; Petrauskas, S.; Valickas, R.; Wolfgramm, M.; Huenges, E. Approach to develop a soft stimulation concept to overcome formation damage—A case study at Klaipeda, Lithuania. In *Proceedings of the 42nd Workshop on Geothermal Reservoir Engineering, Stanford, CA, USA, 13–15 February 2017*; Stanford University: Stanford, CA, USA, 2017.
6. Puronas, V. A Reservoir Model and Production Capacity Estimate for Cambrian Geothermal Reservoir in Kretinga, Lithuania. In *Geothermal Training Programme*; Reports Number 11; United Nations University: Shibuya, Japan, 2002; pp. 187–204.
7. Zinevicius, F.; Sliaupa, S. Lithuania-Geothermal Energy Country Update. In Proceedings of the World Geothermal Congress 2010, Bali, Indonesia, 25–29 April 2010.
8. Zuzevičius, A.; Jurevičius, A.; Galčiuvienė, K. The Geoenvironmental Impact of Klaipėda Geothermal Plant. *J. Environ. Eng. Landsc. Manag.* **2011**, *19*, 304–315. [CrossRef]
9. Suveizdis, P.; Rasteniene, V.; Zui, V. Geothermal field of the Vydmantai-1 borehole within the Baltic heat flow anomaly. *Baltica* **1997**, *10*, 38–46.
10. Guinot, F.; Marnat, S. Death by Injection: Reopening the Klaipėda Geothermal Cold Case. In *Proceedings of the 46th Workshop on Geothermal Reservoir Engineering, Stanford, CA, USA, 15–17 February 2021*; Stanford University: Stanford, CA, USA, 2021.
11. Brehme, M.; Nowak, K.; Banks, D.; Petrauskas, S.; Valickas, R.; Bauer, K.; Burnside, N.; Boyce, A. A Review of the Hydrochemistry of a Deep Sedimentary Aquifer and Its Consequences for Geothermal Operation: Klaipeda, Lithuania. *Geofluids* **2019**, *2019*, 4363592. [CrossRef]
12. Brehme, M.; Regenspurg, S.; Leary, P.; Bulut, F.; Milsch, H.; Petrauskas, S.; Valickas, R.; Blöcher, G. Injection-Triggered Occlusion of Flow Pathways in Geothermal Operations. *Geofluids* **2018**, *2018*, 4694829. [CrossRef]
13. Klimas, A.A.; Gregorauskas, M.; Malisauskas, A. Computer Models, Used for Klaipeda Geothermal Plant Operation Failures Analyse. *Rigas Teh. Univ. Zinat. Rak.* **2010**, *45*, 7–15.
14. Petrauskas, S.; Šliaupa, S.; Nair, R.; Valickas, R. *The Horizon 2020 SURE Project: Deliverable 6.1: Report on a Field Scale RJD Stimulation for the Klaipeda Site*; GFZ German Research Centre for Geosciences: Potsdam, Germany, 2019.
15. Radeckas, B.; Lukosevicius, V. Klaipeda Geothermal Demonstration Project. In Proceedings of the World Geothermal Congress 2000, Kyushu-Tohoku, Japan, 28 May–10 June 2000.
16. Šliaupa, S.; Motuza, G.; Korabliova, L.; Ciuraite, K.; Puronas, V. Geothermal potential of hot granites of Lithuania. In Proceedings of the World Geothermal Congress 2010, Bali, Indonesia, 25–29 April 2010.
17. Šliaupa, S.; Zinevičius, F.; Mazintas, A.; Petrauskas, S.; Dagilis, V. Geothermal Energy Use, Country Update for Lithuania. In Proceedings of the European Geothermal Congress, Den Haag, The Netherlands, 11–14 June 2019.
18. Šliaupa, R.S.; Zuzevičius, A.; Rastenienė, V.; Baliukevičius, A.; Zinevičius, F.; Gudzinskas, J. Vakarų Lietuvos Regione Esančių Geoterminės Energijos Resursų Potencialo Išaiškinimas ir Pagrindimas, bei Galimybės jų Panaudojimui Energijos Gamybai. 2008. Available online: https://enmin.lrv.lt/uploads/enmin/documents/files/Veikla/Veiklos%20sritys/Atsinaujinantys%20energijos%20%C5%A1altiniai/Moksliniai-tiriamieji%20darbai/Geotermines_energijos_potencialas.pdf (accessed on 1 January 2025).
19. Suveizdis, P.; Rasteniene, V.; Zinevicius, F. Geothermal Potential of Lithuania and Outlook for Its Utilization. In Proceedings of the World Geothermal Congress 2000, Kyushu-Tohoku, Japan, 28 May–10 June 2000.
20. Zinevicius, F.; Bickus, A.; Rasteniene, V.; Suveizdis, P. Geothermal Potential and First Achievements of its Utilization in Lithuania. In Proceedings of the World Geothermal Congress 2005, Antalya, Turkey, 24–29 April 2005.
21. Zinevicius, F.; Rasteniene, V.; Bickus, A. Geothermal Development in Lithuania. Available online: https://pangea.stanford.edu/ERE/pdf/IGAstandard/EGC/szeged/O-4-07.pdf (accessed on 1 September 2023).
22. Sonnenthal, E.; Spycher, N.; Xu, T.; Zheng, L. TOUGHREACT V4.12-OMP and TReactMech V1.0 Geochemical and Reactive-Transport User Guide. 2021. Available online: https://escholarship.org/uc/item/8945d2c1 (accessed on 1 January 2025).
23. Memon, A.R.; Pal, M. Assessing Geothermal Energy Production Potential of Devonian Geothermal Complexes in Lithuania. *Energies* **2025**, *18*, 612. [CrossRef]
24. T-Navigator-Geothermal Modelling Software from Rock Flow Dynamics. Available online: https://rfdyn.com/solutions/new-energy/ (accessed on 1 January 2025).